Schizosaccharomyces pombe KAT5 contributes to resection and repair of a DNA double strand break

Tingting Li[1], Ruben C. Petreaca[1&2] and Susan L. Forsburg[1&*]

[1]Program of Molecular and Computational Biology, University of Southern California, Los Angeles CA 90089-2910

[2]Department of Molecular Genetics, Ohio State University, Marion OH 43302

*Corresponding author at Forsburg@usc.edu

Keywords: fission yeast, DSB repair, KAT5, Mst1, resection

Abstract

Chromatin remodeling is essential for effective repair of a DNA double strand break. KAT5 (*S. pombe* Mst1, human TIP60) is a MYST family histone acetyltransferase conserved from yeast to humans that coordinates various DNA damage response activities at a DNA double strand break (DSB), including histone remodeling and activation of the DNA damage checkpoint. In *S. pombe*, mutations in *mst1*$^+$ causes sensitivity to DNA damaging drugs. Here we show that Mst1 is recruited to DSBs. Mutation of *mst1*$^+$ disrupts recruitment of repair proteins and delays resection. These defects are partially rescued by deletion of *pku70*, which has been previously shown to antagonize repair by homologous recombination. These phenotypes of *mst1* are similar to *pht1-4KR*, a non-acetylatable form of histone variant H2A.Z, which has been proposed to affect resection. Our data suggest that Mst1 functions to direct repair of DSBs towards homologous recombination pathways by modulating resection at the double strand break.

Introduction

The DNA damage response choreographs multiple cellular activities such as lesion detection, activation of the DNA damage checkpoint, break repair, and recovery (rev. in (Langerak and Russell 2011)). Chromatin remodeling is central to the faithful execution of these processes, requiring the coordination of histone modifiers, remodelers, and chromatin assembly factors (rev. in (Bakkenist and Kastan 2015; Clouaire and Legube 2019; Aleksandrov *et al.* 2020)). Acetylation of histone H4 is one marker associated with chromatin remodeling at a double strand break (DSB), a potentially lethal form of DNA damage. There is good evidence that histone H4 acetylation is linked to radioresistance and the repair response, possibly by facilitating chromatin mobilization (rev. in (Dhar *et al.* 2017; Van and Santos 2018)).

The MYST family of histone acetyltransferases (HATs) is defined by a distinct catalytic domain, and its members are implicated in histone acetylation at DSBs (rev. in (Utley and Côté 2003; Thomas and Voss 2007)). KAT5 is the most highly conserved HAT of this family, known as Mst1 in *S. pombe,* Esa1 in *S.*

cerevisiae, and TIP60 in mammals (rev. in (Avvakumov and Côté 2007; Pillus 2008)). The gene is essential for viability in all species, because in addition to its role in DSB repair it performs other functions such as transcriptional regulation, heterochromatin assembly and centromere assembly (rev. in (Pillus 2008)). In humans, TIP60 has also been identified as a tumor suppressor (rev. in (Sapountzi *et al.* 2006; Voss and Thomas 2009) and is a therapeutic target (rev. in (Judes *et al.* 2015)).

KAT5 contains a chromodomain in addition to its HAT domain, which suggests that it binds methylated histones (rev. in (Utley and Côté 2003; De La Cruz *et al.* 2005)). KAT5 functions in the context of a large protein complex called NuA4, and acetylates numerous substrates including histones H2A, H3, and H4, and the histone variants H2A.X and H2A.Z (Kimura and Horikoshi 1998; Smith *et al.* 1998; Allard *et al.* 1999; Galarneau *et al.* 2000; Babiarz *et al.* 2006; Keogh *et al.* 2006). Evidence from human cells has shown that KAT5 can acetylate non-histone proteins as well, including the checkpoint kinase ATM and the tumor suppressor TP53 (Sun *et al.* 2005; Jiang *et al.* 2006; Leduc *et al.* 2006; Sykes *et al.* 2006; Tang *et al.* 2006; Kim *et al.* 2007; Naidu *et al.* 2012; Ortega-Atienza *et al.* 2016). Importantly, NuA4 cooperates with the Swr1 chromatin remodeler that is required for exchange of histone H2A with the variant H2A.Z ((rev. in (Scacchetti and Becker 2021) (Kobor *et al.* 2004; Krogan *et al.* 2004; Keogh *et al.* 2006; Zhou *et al.* 2010)).

Evidence from both yeast and humans shows that the NuA4 complex is recruited to DSBs by multiple binding partners including phosphorylated H2A(X) (Downs *et al.* 2004), methylated histone H4K20 (Jacquet *et al.* 2016), methylated histone H3K36 (Li and Wang 2017), methylated histone H3K9 via the KAT5 chromodomain (Sun et al. 2005; Sun et al. 2009, Ayrapetov et al. 2014), and interaction with Nbs1, a component of the end-binding resection complex MRN (Cheng *et al.* 2018b). In fission yeast, physical association between KAT5/SpMst1 and the homologous recombination protein Rad52 has also been demonstrated (Gómez *et al.* 2008). However, how these recruiting partners cooperate or compete with each other is unknown.

Recruitment of the NuA4 complex to the sites of DSBs has several outcomes. There is evidence that the recruitment of variant H2A.Z and its subsequent acetylation by KAT5 are an essential early step in the DNA damage response (Morillo-huesca *et al.* 2010; Papamichos-Chronakis *et al.* 2011; Xu *et al.* 2012; Gursoy-Yuzugullu *et al.* 2015). H2A.Z must be acetylated and then removed so that KAT5 can acetylate H4 (Bird *et al.* 2002; Downs *et al.* 2004; Doyon *et al.* 2004; Murr *et al.* 2005; Clarke *et al.* 2017). Acetylation of the damage specific phosophorylated histone variant γ-H2A(X) promotes its turnover (Ikura *et al.* 2007; Jha *et al.* 2008; Sharma *et al.* 2010; Soria *et al.* 2012). There is also evidence that NuA4 acetylates the ssDNA binding protein RPA, to regulate resection (Cheng et al. 2018; Kobayashi et al. 2010; Xu et al. 2010). This activity may be important to activate the homologous recombination pathway as opposed to other types of repair (Renaud *et al.* 2015; Jacquet *et al.* 2016).

In fission yeast, Mst1 has multiple activities in chromosome structure, heterochromatin assembly, centromere function, and transcription (Minoda *et al.* 2005; Gómez *et al.* 2008; Kim *et al.* 2009; Nugent *et al.* 2010; Xhemalce and Kouzarides 2010). Previously, we showed that a temperature sensitive mutation *mst1*^{ts} (*mst1*Δ *nmt:mst1-L344S*) results in sensitivity to DNA damaging agents even at permissive temperatures (Gómez et al. 2008; Gómez, Espinosa, and Forsburg 2005). Although we showed that *mst1*$^{+}$ affects transcription of a variety of genes, changes in expression do not appear sufficient to account for its DNA damage sensitivity (Nugent *et al.* 2010). Here, we present evidence that *mst1*$^{+}$ affects DSB repair in fission yeast. We show that Mst1 is recruited to DSB. *mst1-L344S* cells show defects in recruiting downstream factors including Rad52 and RPA. Interestingly, this phenotype is partially rescued by deletion of the end-binding protein Pku70, normally required for NHEJ repair. Our data suggest that Mst1 contributes to efficient resection. Finally, a non-acetylatable H2A.Z mutant (*pht1-4KR*) phenocopies *mst1-L344S*, indicating that H2A.Z may be an important substrate for this effect.

Materials and methods

Strains and Media

Fission yeast cells were grown in YES (yeast extract with supplements) or PMG (pombe minimal glutamate) with appropriate supplements (Sabatinos and Forsburg 2010). Yeast strains used in this research are listed in Supplementary table S2 in the supplemental material.

Serial Dilution plating

Yeast cell cultures were grown at 25ºC in YES for two days. Cultures were diluted in YES to equal concentrations. Five-fold serial dilutions of the cultures were then spotted onto YES plates containing different concentrations of drugs. Plates were incubated at 25ºC or 32ºC for the time indicated in each figure legend.

Determination of DSB-induced recombination rates

DSB-induced recombination outcomes were determined using the strain *ade6-M26 int::pUC8/ura4+/MATa/ade6-L469* described in (Schuchert and Kohli 1988; Fortunato *et al.* 1996). The *S. cerevisiae* homothallic endonuclease (HO) was expressed on a plasmid from the *nmt1* promoter. Cells were first grown up in PMG (pombe minimal glutamate) liquid media lacking uracil and thiamine (PMG -ura -thia) for two days. Cell cultures were then plated onto PMG -ura -leu +thia agar media for five days at 25ºC. After the five-day incubation, colonies were then streaked onto PMG -leu -thia agar media and incubated at 25ºC for seven days (HO expression induced). Three colonies from each induced-break plate were then selected and serially diluted 1:100 in sterile MilliQ H2O. 100µl of the diluted cultures was plated onto PMG low ade -leu -thia agar media. Agar plates were incubated at 25ºC. After the 14-day incubation, red, white and red/white half sectored colonies were counted and marked. Plates were then replica plated onto PMG -leu -ade -thia and PMG

100 -ade, -ura -thia and allowed to grow for another six days at 25ºC before counting colonies with each phenotype.
101 At least three biological replicates were performed. About 8% are likely "complex" rearrangement, for
102 example colonies that were red/white half sectored on PMG low ade -leu -thia agar media. These colonies arise
103 from recombination intermediates that were not repaired before replication (Fortunato *et al.* 1996).

104 **Live-cell imaging and Quantitative Measurements**

105 Live cells imaging was performed as described in (Green *et al.* 2015). Yeast cell cultures were grown
106 at 25ºC in YES overnight. Cells were transferred into PMG + HULAA (Histidine, Uracil, Leucine, Adenine,
107 Arginine) liquid cultures at 25ºC for 16 hours before treating with the indicated drugs for four hours. Cells
108 were collected at OD_{595} 0.3 -0.6, concentrated by centrifuging 1ml at 1500g for 1min and resuspended in 40µl.
109 Concentrated cells were placed on a thin-film pad of 2% agarose in PMG+HULAA on a glass slide. A coverslip
110 was added. Live cells were imaged on DeltaVision Core microscope with softWoRx v4.1 (GE, Issaquah, WA),
111 using a 60X lens, and then deconvolved and projected in softWoRx software. Images were acquired in 13
112 0.2µm z-sections, then deconvolved and Maximum Intensity Projected (softWoRx, default settings). Two
113 separate fields were imaged in each experiment, and 2 to 4 biological replicates were assessed for consistency.
114 Images for publication were contrast adjusted using an equivalent histogram stretch on all samples. Color
115 balance was adjusted, and scale bars were added in Fiji (Schindelin *et al.* 2012). Significance was calculated
116 using the Mann-Whitney U test.

117 **LacO LacI-mCherry DSB array colocalization with CFP-tagged Rad52**

118 Co-localization was performed as described in (Yu *et al.* 2013). Cells were cultured at 25ºC in PMG +
119 HULAA (Histidine, Uracil, Leucine, Adenine, Arginine) +Thiamine liquid media to OD_{595} of 0.4-0.6. Cells
120 were then washed twice with PMG +HULAA medium and incubated at 25ºC for 19 hours to induce HO-driven
121 DSB break. Following induction, cells were collected at OD_{595} of 0.3 to 0.6, and were processed and imaged
122 as described above.

123 **Chromatin Immunoprecipitation (ChIP) assay**

124 Chromatin immunoprecipitation (ChIP) was performed as in (Du *et al.* 2006). Cells were grown in
125 PMG+HULAA+Thiamine overnight to OD_{595}~0.6. Cells were washed 3 times with EMM+HULAA and
126 released in PMG+HULAA-Thiamine at 32ºC with shaking. Samples were taken after right after washing into
127 PMG+HULAA-Thiamine (T=0), 22hrs(T=22), 24hrs (T=24) and 26hrs (T=26). All samples were fixed with
128 1% formaldehyde for 20min followed by 5 minutes quenching with Glycine. Cells were lysed in standard ChIP
129 buffer and immunoprecipitations were set up using antibodies against GFP (Abcam290), V5(Abcam15828).
130 DNA was column purified using a Qiagen PCR purification kit and qPCR was performed. Fold enrichment
131 was calculated as 100*2^(Adjusted 100% INPUT – Ct(IP)).

132 **Western Blots**

133 For the time course experiment, cells were grown at 32ºC in YES to OD_{595}~0.6 then treated with 40μM
134 camptothecin for 4hrs. Cells were washed three times with YES, then released in YES without drug. Time
135 points were taken at T=0 (before addition of drug), T=4 (after 4hrs of drug treatment), and T=6, 8 (two and
136 four hours after removal of drug). Cells were lysed in 20% TCA. Antibodies against phosphorylated H2A
137 (Abcam 17353) and control PCNA (Santa Cruz-56 PC10) were used. For the Chk1-HA phosphorylation
138 experiment, cells were grown at 32ºC in YES to OD_{595}~0.6 then treated for 4hrs with 40μM camptothecin,
139 15mM HU or 0.01%MMS then cells were processed as described above. An anti-HA antibody (12CA5
140 Abcam16918) was used.
141
142 **Results**
143 **Mst1 is important for double-strand break repair in *S. pombe***
144 Mst1 homologs in mammalian cells (TIP60) and *S. cerevisiae* (*ESA1*) are known to be important for
145 DSB repair (rev. in (Ghobashi and Kamel 2018; Van and Santos 2018; Clouaire and Legube 2019; Aleksandrov
146 *et al.* 2020)). We have previously shown that a *S. pombe mst1*$^+$ temperature sensitive allele (*mst1-L344S*)
147 renders cells sensitive to various DNA damaging drugs (Gómez *et al.* 2008). Here we expand these studies to
148 further dissect the role of *mst1*$^+$ in DSB repair.
149 Our original *mst1-L344S* construct is expressed from the *nmt1* promoter inserted at the *leu1*$^+$ locus in
150 a deletion background (*mst1*Δ *nmt:mst1-L344S* Gómez et al. 2008) but subsequently, the same allele was
151 engineered at the native locus under control of the endogenous *mst1*$^+$ promoter (*mst1-L344S* Garabedian et al.
152 2012). We tested the sensitivity of both versions to bleomycin, which creates single and double strand DNA
153 breaks (Stubbe and Kozarich 1987; Burger 1998). Both these strains were modestly sensitive to the drugs at
154 25ºC (Figure 1A; Gómez et al. 2008), consistent with a requirement for Mst1 in DSB repair. Because the newer
155 *mst1-L344S* allele does not generate autofluorescence to the same extent as our original allele, we employed it
156 here for visual assays.
157 We investigated the role of *mst1*$^+$ in repair of a single DSB break. We first utilized a strain that uses
158 the homothallic switching endonuclease (HO) to induce a single DSB between two non-tandem repeats as
159 originally described by (Schuchert and Kohli 1988) and modified by (Osman *et al.* 2000) (Figure 1B). In this
160 strain, a functional *ura4*$^+$ gene is flanked by two full length non-functional *ade6* alleles, each containing a
161 different point mutation. The HO endonuclease makes a DSB at *MATa* site adjacent to *ura4*$^+$. The repair
162 outcomes can be determined by selecting Ade^+ cells and screening for Ura^+ (Fortunato *et al.* 1996; Osman *et*
163 *al.* 1996, 2000; Ahn *et al.* 2005). Uracil auxotrophic colonies ("deletion type", whether Ade^+ or Ade^-) result
164 from deletion and rearrangement, in which cells repaired the lesion by Single Strand Annealing (SSA), Non-

165 Homologous End-Joining (NHEJ), or more complex rearrangements. In contrast, Ade$^+$ colonies that retain
166 Ura+ ("conversion type") are presumed to derive from gene conversion via homologous recombination.
167 Following induction of the DSB, we observed that the survival of *mst1-L344S* was much lower than
168 the survival in wild-type cells (Figure 1C), consistent with a repair defect. In wild-type cells, about 55.64% of
169 colonies are deletion type (Ade+/Ade- Ura-) while 36.70% of colonies were conversion type (Ade+ Ura+)
170 (Figure 1D). In the surviving *mst1-L344S* cells, we observed a significantly higher percentage of colonies
171 showing deletion-type repair (75.3%) than in wild type (Figure 1D). These data suggest that wild type *mst1*$^+$
172 biases repair towards conversion-type, error-free recombination.
173 To examine whether Mst1 physically localizes to DSB breaks as has been reported for *Hs*TIP60 and
174 *Sc*Esa1 (Downs and Jackson 2004; Sun *et al.* 2009), we employed a strain previously engineered to test
175 recruitment of proteins by ChIP to one single double strand break (Figure 1E) (Du *et al.* 2006). This assay can
176 monitor both temporal and spatial recruitment of proteins to a single DSB. We detected Mst1 localized near
177 the DSB after induction, although the level of enrichment was lower than that of Rad52 (Figure 1E, note two
178 different Y-axes for Mst1 and Rad52). As expected, Mst1 localization to sequences near DSB was reduced in
179 cells missing H3K9 methyltransferase Clr4, which is consistent with previous finding that *Hs*TIP60 binds to
180 the DSB via H3K9^{me} (Sun et al. 2005; Sun et al. 2009, Ayrapetov et al. 2014). Additionally, Rad52 localization
181 to the DSB was reduced in *clr4*Δ (Figure 1E, supplementary figure S1), consistent with findings in human cells
182 that H3K9^{me}-deficient cells had reduced homologous recombination-mediated repair (Ayrapetov *et al.* 2014).
183 **Mst1 contributes to recruitment of repair factors to DSBs**

184 Consistent with a role for Mst1 in DSB repair, we found that the mutant *mst1* at permissive temperature
185 is modestly sensitive to agents that induce DSBs, including the radiomimetic drugs Bleomycin and its analogue
186 Phleomycin (Belenguer et al. 1995) (Figure 1A, supplementary figure 2), suggesting this mutant has attenuated
187 function even under permissive conditions. We next examined the recruitment of homologous recombination
188 proteins in *mst1-L344S* cells using a visual screen following treatment with phleomycin. First, we looked at
189 the localization of RPA and Rad52 proteins (Figure 2A, supplementary table 1). Untreated wild type and *mst1*
190 cells had a similar percentage of cells with foci. However, following phleomycin treatment, we observed
191 significantly more cells with foci in wild type than in *mst1-L344S* cells. We also imaged cells with GFP-tagged
192 Rad54, a recombination protein that acts downstream of Rad52 (Figure 2B; Onaka et al. 2016). Similar to RPA
193 and Rad52, the fraction of *mst1-L344S* cells with Rad54 foci was lower than in the wild type strain (Figure
194 2B, supplementary table 1). These observations suggest that Mst1 is required for the normal recruitment of
195 downstream HR factors.
196 Next, we examined the recruitment of Rad52 at a single, induced DSB site. We utilized a strain that
197 contains an HO-inducible DSB adjacent to a lacO array that recruits mCherry-lacI, and CFP-tagged Rad52

198 (Yu *et al.* 2013). We imaged both wild-type and *mst1-L344S* cells over a four-hour period. In wild-type cells,
199 we observed that 75% of total Rad52 foci co-localize with mCherry signal until 100 minutes (Figure 2C top).
200 After 100 minutes, the percentage of colocalization dropped in wild type, because the mCherry-LacI signal
201 disappears (Figure 2C bottom and Figure 2D). This loss of mCherry-lacI likely reflects resection at DSBs that
202 eliminates the LacO target, as shown previously (Yu *et al.* 2013; Leland *et al.* 2018). Consistent with these
203 prior reports, we observed that the mCherry-DSB foci dropped to 25% by the end of four-hour time-course
204 (Figure 2D, Yu et al. 2013). In contrast, in *mst1-L344S* cells, fewer than 40% of total Rad52 foci colocalize
205 with mCherry-DSB foci across the four-hour time-course, suggesting Mst1 is involved in Rad52 recruitment
206 (Figure 2C top). Strikingly, however, over 90% of mCherry-DSB signal remained even at the end of the time-
207 course (Figure 2C bottom and Figure 2D). This suggests that in the absence of functional Mst1, resection is
208 inhibited, so the LacI-mcherry bound to the lacO array persists.

209 **Processing of DSBs and a role for Ku**

210 The heterodimeric Ku complex is very abundant and binds rapidly and immediately to DSBs (Fell and
211 Schild-Poulter 2015; Shibata *et al.* 2018). Ku inhibits initial resection driven by MRN, while MRN removes
212 Ku to promote proper resection and facilitate homologous recombination (HR) (Tomita *et al.* 2003; Langerak
213 *et al.* 2011; Shao *et al.* 2012; Myler *et al.* 2017; Shibata *et al.* 2018). Unexpectedly, we found that *pku70*Δ
214 partially rescues the bleomycin sensitivity of *mst1*Δ *mst1-L344S* (Figure 3A).

215 We wondered whether Pku70 also affects the recruitment of repair proteins in *mst1-L344S*, so we
216 imaged fluorescently tagged RPA under phleomycin treatment. We observed first that the percentage of
217 untreated cells with RPA foci in *pku70*Δ and *pku70*Δ *mst1-L344S* is higher than in wild type or *mst1-L344S*
218 (Figure 2A, supplementary figure 3, supplementary table 1), suggesting a burden of endogenous damage.
219 However, cell growth and cell length at septation were not significantly affected (Figure 3A, supplementary
220 figure 4).

221 Upon treatment, the number of positive cells is only slight increased, and does not reach the level
222 observed in wild-type cells (Figure 2A, supplementary figure 3A, supplementary table 1). Results were slightly
223 different for Rad52: the *pku70*Δ single mutant cells showed a comparable level to wild type in untreated
224 conditions, with little change following treatment. The untreated double mutant *pku70*Δ *mst1-L344S* were
225 higher than either single mutant and showed a modest increase upon treatment, but not to the levels of wild
226 type (Figure 2A, supplementary figure 3A, supplementary table 1). Finally, the fraction of *pku70*Δ with Rad54
227 foci is similar to wild type in untreated cells, increased by the same relative proportion following treatment.
228 Again, the untreated *mst1-L344S pku70*Δ has a higher baseline in untreated cells than either single mutant, and

229 induces to approximately wild type levels (Figure 2B, supplementary figure 3C, supplementary table 1).

230 We used the mCherry-LacI marked HO-induced DSB system to examine the apparent resection of DSB
231 in *pku70*Δ mutants by monitoring the disappearance of mCherry signal (Figure 2D). We find that *pku70*Δ
232 single mutant cells do show a slight reduction in mCherry-DSB foci over time, but this effect is far more
233 modest than that in wild-type. At the end of the time-course, just under 70% of the *pku70*Δ cells still contain
234 mCherry-DSB foci. We observed a similar phenotype in *pku70*Δ *mst1-L344S* cells. (Figure 2D).

235 Long range resection is initiated by MRN and extended by the exonuclease Exo1, as well as other
236 proteins (Zhu *et al.* 2008; Langerak *et al.* 2011; Yan *et al.* 2019). We observed that mCherry-LacI marked
237 DSBs do not disappear over the time-course in *exo1*Δ, in contrast to wild-type (Figure 2D), and consistent with
238 a failure in resection. We observed that *exo1*Δ*, mst1-L344S,* and the double mutant *exo1*Δ *mst1-L344S* all show
239 a similar persistence of the mCherry signal. Additionally, *exo1*Δ *mst1-L344S* has similar sensitivity to
240 bleomycin as the *mst1-L344S* single mutant and this sensitivity is rescued by *pku70*Δ (Figure 3A). These data
241 suggest that $mst1^+$ and $exo1^+$ are in the same pathway.

242 **Is H2A.Z a target of Mst1 to regulate DSB repair**?

243 In other organisms that the presence and turnover of the histone variant H2A.Z (*S. pombe* Pht1), a
244 KAT5 substrate, is important for the proper repair of DSBs by regulating resection (Xu *et al.* 2012; Gursoy-
245 Yuzugullu *et al.* 2015; Jiang *et al.* 2015). In human cells, H2A.Z depletion leads to higher ssDNA accumulation
246 and lower DSB recovery from HR (Xu *et al.* 2012; Jiang *et al.* 2015). Failure to remove H2A.Z at DSBs in
247 human cells leads to higher RPA binding and higher recovery from HR (Gursoy-Yuzugullu *et al.* 2015). In
248 fission yeast, H2A.Z is a known substrate of Mst1, and a mutant *pht1-4KR* that disrupts the Mst1 acetylation
249 sites causes genome instability and anaphase defects (Kim *et al.* 2009). To investigate the role of H2A.Z
250 acetylation in repair, we compared the phenotype of *pht1-4KR* and *pht1*Δ to *mst1-L344S.* We observed
251 significant reduction in RPA and Rad52 foci in *pht1-4KR* at 25ºC similar to that observed with *mst1-L344S*
252 cells (Figure 2A, supplementary figure 3B, supplementary table 1). However, in contrast to *mst1-L344S,* the
253 sensitivity to bleomycin we observe in *pht1-4KR* is not rescued by *pku70*Δ (Figure 3B).

254 We also compared the phenotypes of *pht1*Δ and *pht1-4KR* cells. *pht1*Δ showed fewer cells with RPA
255 foci compared to wild type under phleomycin treatment (Figure 2A, supplementary figure 3B, supplementary
256 table 1). Rad52 foci were also reduced in *pht1*Δ compared to wild type under phleomycin treatment (Figure
257 2A). However, the effect of *pht1-4KR* cells was more dramatic than *pht1*Δ*,* and much closer to the observations
258 in *mst1-L344S* (Figure 2A, supplementary table 1). Finally, we used the mCherry-DSB reporter system to

259 examine resection *in vivo*. As with *mst1-L344S* and *exo1*Δ, *pht1-4KR* cells showed a persistent mCherry-DSB
260 signal, consistent with a failure to resect (Figure 2D).

261 **The damage checkpoint is normal in *mst1-L344S***

262 Previously, we showed that the temperature-sensitive allele *mst1*Δ *leu1*$^{+}$*::nmt-mst1-L344S* is sensitive
263 to S-phase specific genotoxins including methyl methanesulfonate (MMS), which causes alkylation damage
264 that inhibits replication, and camptothecin (CPT), a topoisomerase-I inhibitor that causes lesions during S-
265 phase (Wan *et al.* 1999; Fung *et al.* 2002; Morishita *et al.* 2003; Frampton *et al.* 2006). In contrast to our
266 observations with phleomycin, which induces general DSBs, we observed that the percentage of cells with
267 RPA and Rad52 foci was higher in *mst1-L344S* cells treated with these S-phase specific genotoxins than that
268 in wild-type (Figure 4A). This is consistent with these S-phase specific lesions inducing different repair
269 pathways, including post-replication repair via translesion synthesis and template switching to repair MMS-
270 induced damage, as well as nucleolytic cleavage of protein -DNA adducts to repair CPT-induced damages
271 (rev. in (Alagoz et al. 2012; Arbel, Liefshitz, and Kupiec 2020)).

272 We examined genetic interactions between *mst1-L344S* and mutants that affect checkpoint under
273 treatment with a variety of S-phase specific genome stressors (Supplementary figure 5). A modest growth
274 defect in untreated cells was observed for the double mutant *mst1-L344S rad3*Δ but not for others. In cells
275 treated with UV or MMS at 25ºC, we observed a striking negative interaction between *mst1-L344S* and damage
276 checkpoint mutants *chk1*Δ or *crb2*Δ at 25ºC, suggesting a requirement for an active damage checkpoint
277 response under these treatments. This data is consistent with previous findings in *S. cerevisiae* that the cell
278 cycle delay in NuA4 mutant depends on Rad9 (*Sp*Crb2 ortholog) after DSB induction (Javaheri *et al.* 2006).
279 We treated cells with MMS, CPT or HU and performed western blots against HA tagged Chk1. In wild-type,
280 Chk1 is phosphorylated in cells treated with four-hour CPT or MMS, but not in untreated cells or cells treated
281 with HU (Figure 4B;Walworth and Bernards 1996). We observed a largely similar phosphorylation pattern in
282 *mst1-L344S* mutant (Figure 4B), although there may be a modest reduction in the amount of pChk1. H2A
283 phosphorylation, one of the first sensors of DNA damage and double strand breaks, was also present in *mst1-*
284 *L344S* cells after 4-hour CPT treatment as in wild-type cells and diminished after removing drugs from cell
285 culture (Figure 4C). Mst1 is not required for checkpoint activation in response to S-phase specific lesions but
286 depends on that response for viability.

287

288 **Discussion**

289 The MYST protein Mst1 (hTIP60; ScEsa1; KAT5) is the catalytic subunit of the NuA4 histone
290 acetyltransferase complex, and makes pleiotropic contributions to genome stability (rev. in (Lafon *et al.* 2007;

291 Pillus 2008)). Multiple studies indicate that hTIP60 and ScEsa1 contribute to DSB repair through acetylation
292 (rev. in (Ghobashi and Kamel 2018)), and show that the acetyltransferase binds near DSB regions (Downs *et*
293 *al.* 2004; Sun *et al.* 2009; Xu *et al.* 2010; Li and Wang 2017; Cheng *et al.* 2018). The budding yeast ScEsa1
294 acetylates ssDNA binding protein RPA at DSBs (Cheng *et al.* 2018) and in mammalian cells, TIP60 promotes
295 HR localization of recombination protein Rad51 (Murr *et al.* 2005).

296 Previously we showed that Mst1 is *S. pombe* is essential for viability and we demonstrated the
297 temperature sensitive allele *mst1-L344S* is sensitive to a number of genotoxins (Gómez et al. 2008; Gómez,
298 Espinosa, and Forsburg 2005). Here, we confirmed that Mst1 in *S. pombe* is important for DSB repair because
299 both temperature sensitive alleles are sensitive to a DSB-inducing environment including treatment with
300 phleomycin or bleomycin, or constitutive HO-nuclease expression (Figure 1A, 1C, 3 and supplementary figure
301 2). We find that Mst1 directly localizes to DSBs, and this localization depends on H3K9^{me} (Figure 1E and
302 Figure 5). We observe that even under permissive growth conditions, *mst1-L344S* shifts the balance of repair
303 away from HR towards SSA or NHEJ (Figure 1D). We also observed that a lower percentage of *mst1-L344S*
304 cells compared to wild type show visible foci of HR associated proteins RPA, Rad52 or Rad54, following
305 treatment with DSB inducing agents (Figure 2A, B). Together, these observations suggest that Mst1 facilitates
306 homologous recombination to repair DSBs, and in its absence, HR is impaired (Figure 5).
307 There are conflicting data as to whether KAT5/NuA4 influences non-homologous end joining (NHEJ),
308 which is typically the alternative pathway for repair if HR is inhibited (Chang *et al.* 2017). In budding yeast,
309 ScEsa1 has been reported to be essential for NHEJ at DSBs (Bird *et al.* 2002). However, studies in mammalian
310 cells suggest TIP60 instead inhibits NHEJ by acetylating H2A and H4; this reduces loading of 53BP1 protein
311 that promotes NHEJ (Tang *et al.* 2013; Renaud *et al.* 2015; Jacquet *et al.* 2016). Consistent with this, in
312 budding yeast deletion of the 53BP1 orthologue Sc*rad9* increases resection efficiency (Bonetti *et al.* 2015) and
313 similarly, fission yeast *crb2*Δ mutants have increased resection (Leland *et al.* 2018). However, in fission yeast,
314 the G2-dominant cell cycle means that NHEJ is generally not the preferred pathway for DSB repair in growing
315 cells (rev. in (Langerak and Russell 2011)). Because of this, we did not specifically examine efficiency of
316 NHEJ. Our data suggest that Mst1 affects homologous recombination, specifically by reducing long-range
317 resection (Figure 2 and Figure 5).
318 To monitor resection, we used a visual assay in which a lacO array marked by lacI-mCherry is adjacent
319 to an induced double strand break. Previous studies have shown that loss of the lacO array adjacent to a break
320 correlates with resection (Yu *et al.* 2013; Leland *et al.* 2018). Consistent with this, we find that the mCherry
321 signal declines over time in a wild type in the presence of the induced break, but not in an *exo1*Δ mutant that
322 lacks the long-range exonuclease. We also observe that *mst1-L344S* resembles *exo1*Δ in this assay. The data

323 from this, as well as the mutant sensitivity to DSB-inducing drugs, suggest that *mst1* and *exo1* are in a common
324 epistasis group (Figure 5).

325 The end-binding protein complex Ku inhibits resection and thus, homologous recombination (rev. in
326 (Shibata, Jeggo, and Löbrich 2018)). Its activity is coordinated with the Mre11-Rad50-Nbs1 (MRN) complex
327 associated with early steps in resection (rev. in (Shibata, Jeggo, and Löbrich 2018; Syed and Tainer 2018)).
328 While Ku inhibits resection driven by MRN, MRN removes Ku to facilitate homologous recombination (HR)
329 over NHEJ (Langerak and Russell 2011; Shao *et al.* 2012; Myler *et al.* 2017; Shibata *et al.* 2018). Previous
330 work has shown that *pku70*Δ rescues some resection in the absence of the MRN complex (Tomita *et al.* 2003;
331 Langerak *et al.* 2011; Teixeira-Silva *et al.* 2017). Consistent with these observations, we found *pku70*Δ also
332 partially rescues *mst1* and *mst1 exo1*Δ sensitivity to DSB-inducing agents, and partly restores recruitment of
333 HR proteins and resection. This agrees with a model that Pku70 inhibits an alternative resection pathway that
334 is independent of MRN, Mst1, or Exo1.

335 However, we observe an intermediate effect of Pku70 on resection in our visual assay: unexpectedly
336 *pku70*Δ showed stabilization of the mCherry-LacI signal in both wild type and *mst1-L344S* backgrounds,
337 whereas we expected at least the single mutant to show wild type levels of resection. Since Pku70 represses
338 microhomology-mediated end joining (MMEJ), one possibility is that an increase of MMEJ antagonizes
339 resection directly (Decottignies 2007; Wang and Xu 2017). Ku also plays a role in telomere maintenance
340 (Baumann and Cech 2000; Manolis *et al.* 2001), in replication fork restart (Teixeira-Silva *et al.* 2017), and in
341 rDNA stability (Miyoshi *et al.* 2009; Sánchez and Russell 2015). It represses chromosome rearrangements
342 (Prudden *et al.* 2003). We observed increased RPA signal in the *pku70*Δ mutant without any treatment,
343 suggesting the loss of Pku70 causes an increased burden of ssDNA. It is possible that efficiency of resection
344 at a single engineered break is reduced due to recruitment of resection activities to numerous other sites of
345 genotoxic stress that are the result of Ku depletion, but this observation will require further analysis.

346 Multiple studies show the presence and the turnover of the histone variant H2A.Z (SpPht1) is required
347 for DSB repair (Kalocsay *et al.* 2009; Xu *et al.* 2012; Gursoy-Yuzugullu *et al.* 2015; Jiang *et al.* 2015). In
348 mammalian cells, the absence of H2A.Z leads to more ssDNA accumulation and reduced Pku70 localization
349 (Xu *et al.* 2012; Gursoy-Yuzugullu *et al.* 2015). Exchange of H2A.Z is required for H4 acetylation by TIP60,
350 which creates open chromatin (Gursoy-Yuzugullu, Ayrapetov, and Price 2015; Xu et al. 2010, 2012). Several
351 acetyltransferases have been implicated in H2A.Z acetylation including KAT5 (Mst1) and KAT2A (Gcn5)
352 (Kusch *et al.* 2004; Babiarz *et al.* 2006; Keogh *et al.* 2006; Millar *et al.* 2006; Zlatanova and Thakar 2008;
353 Kim *et al.* 2009; Semer *et al.* 2019). In mammalian cells, the deposition of H2A.Z precedes its acetylation (Xu
354 *et al.* 2012), while in Drosophila, the acetylation of H2A.Z homolog H2Av stimulates its removal after DNA

355 damage (Kusch *et al.* 2004). Blocking TIP60 prevents both H2A.Z exchange and H4 acetylation (Morillo-
356 huesca *et al.* 2010; Papamichos-Chronakis *et al.* 2011; Xu *et al.* 2012; Shastri *et al.* 2018).
357 To investigate whether H2A.Z acetylation by Mst1 influences repair, we used a non-acetylable mutant
358 of H2A.Z, *pht1-4KR*. This mutation has previously been shown to disrupt Mst1 acetylation sites and leads to
359 chromosome segregation errors (Kim *et al.* 2009). We saw a similar percentage of *pht1-4KR* cells with RPA
360 and Rad52 foci as seen in *mst1-L344S* cells in treated cells, both significantly lower than that in wild type.
361 Additionally, mCherry-DSB foci in *pht1-4KR* did not disappear across the time-course, and the percentage of
362 mCherry-DSB persistence was similar to that in *mst1-L344S* (Figure 2D). This suggests that *pht1-4KR* and
363 *mst1-344S* affect in a common pathway required for resection. We speculate that *pht1-4KR* once inserted
364 cannot be efficiently removed, and interferes with H4 acetylation and chromatin decompaction. This would
365 essentially lock the chromatin in a form refractory to long range resection. This could explain why sensitivity
366 of *pht1-4KR* to DSBs is more severe than that of *pht1*Δ, suggesting that an immobile H2A.Z is more damaging
367 than no H2A.Z at all. However, in contrast to *mst1*, *pht1-4KR* sensitivity to bleomycin is not rescued by *pku70*Δ
368 (Figure 3B). This might suggest that H2A.Z binds to DSBs after Pku70 is removed, but that would be
369 inconsistent with work in mammalian cells suggesting that Ku-recruitment is H2A.Z dependent (Xu *et al.*
370 2012). Further work will be required to resolve these observations.

371 Finally, we show that the temperature sensitive allele *mst1*Δ *leu1*$^{+}$*::nmt:mst1-L344S* is sensitive to S
372 phase specific genotoxins including methyl methanesulfonate (MMS) and camptothecin (CPT) even at
373 permissive temperature (Gómez et al. 2008). This is consistent with a recent study showing that Mst1 in *S.*
374 *pombe* is important for CPT-induced damge repair (Noguchi *et al.* 2019). Studies in *S. cerevisiae* showed
375 Esa1's importance to MMS-induced damage repair through translesion synthesis and sister chromatid
376 recombination (Bird *et al.* 2002; House *et al.* 2014; Renaud-Young *et al.* 2015). Compromised DNA damage
377 repair could be the result of defective damage checkpoint activation. In mammalian cells, TIP60 is known to
378 acetylate ATM and p53 (Sun *et al.* 2005; Sykes *et al.* 2006; Tang *et al.* 2006). However, we find that the
379 temperature sensitive allele does not affect activation of DNA damage checkpoint Chk1 or phosphorylation of
380 H2A(X) (Figure 4B and C).
381 Taken together, our data suggest that SpMst1contributes to repair of a variety of DNA lesions. As in
382 other organisms, our data show that Mst1 acetyltransferase has a particular role in double strand break repair,
383 where it facilitates homologous recombination by promoting long range resection and antagonizing NHEJ-
384 promoting factors such as Ku (Figure 5). Our data suggest that this depends on acetylation of H2A.Z. The
385 conservation of function of this acetyltransferase across eukaryotes indicates the fundamental nature of
386 chromatin modification in DNA repair transactions.
387

Acknowledgement

We would like to thank Li-Lin Du, Michael Keogh, Takuro Nakagawa, Eishi Noguchi, Mathew O'Connell, and Simon Whitehall for strains. We thank Ji-Ping Yuan and Amanda Jensen for assistance and technical support. We are grateful to current members of the Forsburg lab for many helpful comments and discussions throughout the course of the study. This work was supported by NIH R35 GM118109 (SLF).

394 **References**

395 Ahn J. S., F. Osman, and M. C. Whitby, 2005 Replication fork blockage by RTS1 at an ectopic site promotes
396 recombination in fission yeast. EMBO J. 24: 2011–2023. https://doi.org/10.1038/sj.emboj.7600670
397 Alagoz M., D. C. Gilbert, S. El-Khamisy, and A. J. Chalmers, 2012 DNA Repair and Resistance to
398 Topoisomerase I Inhibitors: Mechanisms, Biomarkers and Therapeutic Targets. Curr. Med. Chem. 19:
399 3874–3885. https://doi.org/10.2174/092986712802002590
400 Aleksandrov R., R. Hristova, S. Stoynov, and A. Gospodinov, 2020 The Chromatin Response to Double-
401 Strand DNA Breaks and Their Repair. Cells 9. https://doi.org/10.3390/cells9081853
402 Allard S., R. T. Utley, J. Savard, A. Clarke, P. Grant, *et al.*, 1999 The NuA4 transcription activation/histone
403 H4 acetyltransferase complex contains the essential Esa1 protein as the catalytic subunit and the
404 essential ATM-related cofactor Tra1p. Biochem. Cell Biol. 77: 5108–5119. https://doi.org/10.1139/o99-
405 903
406 Arbel M., B. Liefshitz, and M. Kupiec, 2020 How yeast cells deal with stalled replication forks. Curr. Genet.
407 66: 911–915. https://doi.org/10.1007/s00294-020-01082-y
408 Avvakumov N. ., and J. Côté, 2007 The MYST family of histone acetyltransferases and their intimate links
409 to cancer. Oncogene 26: 5395–5407. https://doi.org/10.1038/sj.onc.1210608
410 Ayrapetov M. K., O. Gursoy-Yuzugullu, C. Xu, Y. Xu, and B. D. Price, 2014 DNA double-strand breaks
411 promote methylation of histone H3 on lysine 9 and transient formation of repressive chromatin. Proc.
412 Natl. Acad. Sci. 111: 9169–9174. https://doi.org/10.1073/pnas.1403565111
413 Babiarz J. E., J. E. Halley, and J. Rine, 2006 Telomeric heterochromatin boundaries require NuA4-dependent
414 acetylation of histone variant H2A.Z in Saccharomyces cerevisiae. Genes Dev.
415 https://doi.org/10.1101/gad.1386306
416 Bakkenist C. J., and M. B. Kastan, 2015 Chromatin perturbations during the DNA damage response in
417 higher eukaryotes. DNA Repair (Amst). 36: 8–12. https://doi.org/10.1016/j.dnarep.2015.09.002
418 Baumann P., and T. R. Cech, 2000 Protection of telomeres by the Ku protein in fission yeast. Mol. Biol.
419 Cell. https://doi.org/10.1091/mbc.11.10.3265
420 Belenguer P., M.-L. Oustrin, G. Tiraby, and B. Ducommun, 1995 Effects of phleomycin-induced DNA
421 damage on the fission yeast Schizosaccharomyces pombe cell cycle. Yeast 11: 225–231.
422 https://doi.org/10.1002/yea.320110305
423 Bird A. W., D. Y. Yu, M. G. Pray-Grant, Q. Qiu, and M. F. Christman, 2002 Acetylation of histone H4 by
424 Esa1 is required for DNA double-strand break repair. Nature 419: 411–415.
425 https://doi.org/10.1038/nature01080.Published
426 Bonetti D., M. Villa, E. Gobbini, C. Cassani, G. Tedeschi, *et al.*, 2015 Escape of Sgs1 from Rad9 inhibition

427 reduces the requirement for Sae2 and functional MRX in DNA end resection . EMBO Rep. 16: 351–
428 361. https://doi.org/10.15252/embr.201439764
429 Burger R. M., 1998 Cleavage of Nucleic Acids by Bleomycin. 2665: 16–19.
430 https://doi.org/10.1021/cr960438a
431 Chang H. H. Y., N. R. Pannunzio, N. Adachi, and M. R. Lieber, 2017 Non-homologous DNA end joining
432 and alternative pathways to double-strand break repair. Nat. Rev. Mol. Cell Biol. 18: 495–506.
433 https://doi.org/10.1038/nrm.2017.48
434 Cheng X., O. Jobin-robitaille, P. Billon, R. Buisson, V. Côté, *et al.*, 2018 Phospho-dependent recruitment of
435 NuA4 by MRX at DNA breaks regulates RPA dynamics during resection. Proc. Natl. Acad. Sci. U. S.
436 A. 6: P93. https://doi.org/10.1186/1756-8935-6-S1-P93
437 Clarke T. L. ., M. P. Sanchez-Bailon, K. Chiang, J. J. . Reynolds, J. Herrero-Ruiz, *et al.*, 2017 PRMT5-
438 Dependent Methylation of the TIP60 Coactivator RUVBL1 Is a Key Regulator of Homologous
439 Recombination. Mol. Cell 65: 900–916. https://doi.org/10.1016/j.molcel.2017.01.019
440 Clouaire T., and G. Legube, 2019 A Snapshot on the Cis Chromatin Response to DNA Double-Strand
441 Breaks. Trends Genet. 35: 330–345. https://doi.org/10.1016/j.tig.2019.02.003
442 Decottignies A., 2007 Microhomology-mediated end joining in fission yeast is repressed by Pku70 and relies
443 on genes involved in homologous recombination. Genetics 176: 1403–1415.
444 https://doi.org/10.1534/genetics.107.071621
445 Dhar S., O. Gursoy-Yuzugullu, R. Parasuram, and B. D. Price, 2017 The tale of a tail: Histone H4
446 acetylation and the repair of DNA breaks. Philos. Trans. R. Soc. B Biol. Sci. 372.
447 https://doi.org/10.1098/rstb.2016.0284
448 Downs J. A., S. Allard, O. Jobin-Robitaille, A. Javaheri, A. Auger, *et al.*, 2004 Binding of chromatin-
449 modifying activities to phosphorylated histone H2A at DNA damage sites. Mol. Cell 16: 979–990.
450 https://doi.org/10.1016/j.molcel.2004.12.003
451 Downs J. A., and S. P. Jackson, 2004 A means to a DNA end: The many roles of Ku. Nat. Rev. Mol. Cell
452 Biol. 5: 367–378. https://doi.org/10.1038/nrm1367
453 Doyon Y., and J. Côté, 2004 The highly conserved and multifunctional NuA4 HAT complex. 2 14: 147–154.
454 https://doi.org/10.1016/j.gde.2004.02.009
455 Doyon Y., W. Selleck, W. S. Lane, S. Tan, and J. Côté, 2004 Structural and functional conservation of the
456 NuA4 histone acetyltransferase complex from yeast to humans. Mol. Cell. Biol. 24: 1884–96.
457 https://doi.org/10.1128/MCB.24.5.1884
458 Du L. L., T. M. Nakamura, and P. Russell, 2006 Histone modification-dependent and -independent pathways
459 for recruitment of checkpoint protein Crb2 to double-strand breaks. Genes Dev. 20: 1583–1596.

460 https://doi.org/10.1101/gad.1422606
461 Fell V. L., and C. Schild-Poulter, 2015 The Ku heterodimer: Function in DNA repair and beyond. Mutat.
462 Res. - Rev. Mutat. Res. 763: 15–29. https://doi.org/10.1016/j.mrrev.2014.06.002
463 Fortunato E. A., F. Osman, and S. Subramani, 1996 Analysis of spontaneous and double-strand break-
464 induced recombination in rad mutants of S. pombe. Mutat. Res. - DNA Repair 364: 147–160.
465 https://doi.org/10.1016/S0921-8777(96)00022-5
466 Frampton J., A. Irmisch, C. M. Green, A. Neiss, M. Trickey, *et al.*, 2006 Postreplication Repair and PCNA
467 Modification in Schizosaccharomyces pombe. Mol. Biol. Cell 17: 2976–2985.
468 https://doi.org/10.1091/mbc.E05
469 Fung A. D., J. Ou, S. Bueler, and G. W. Brown, 2002 A Conserved Domain of Schizosaccharomyces pombe
470 dfp1+ Is Uniquely Required for Chromosome Stability following Alkylation Damage during S Phase.
471 Mol. Cell. Biol. 22: 4477–4490. https://doi.org/10.1128/mcb.22.13.4477-4490.2002
472 Galarneau L., A. Nourani, A. A. Boudreault, Y. Zhang, L. Héliot, *et al.*, 2000 Multiple links between the
473 NuA4 histone acetyltransferase complex and epigenetic control of transcription. Mol. Cell.
474 https://doi.org/10.1016/S1097-2765(00)80258-0
475 Garabedian M. V., C. Noguchi, M. A. Ziegler, M. M. Das, T. Singh, *et al.*, 2012 The double-bromodomain
476 proteins Bdf1 and Bdf2 modulate chromatin structure to regulate S-phase stress response in
477 schizosaccharomyces pombe. Genetics 190: 487–500. https://doi.org/10.1534/genetics.111.135459
478 Ghobashi A. H., and M. A. Kamel, 2018 Tip60 : updates. Hum. Genet. 59: 161–168.
479 Gómez E. B., J. M. Espinosa, and S. L. Forsburg, 2005 Schizosaccharomyces pombe mst2+ encodes a
480 MYST family histone acetyltransferase that negatively regulates telomere silencing. Mol. Cell. Biol. 25:
481 8887–8903. https://doi.org/10.1128/MCB.25.20.8887-8903.2005
482 Gómez E. B., R. L. Nugent, S. Laria, and S. L. Forsburg, 2008 Schizosaccharomyces pombe histone
483 acetyltransferase Mst1 (KAT5) is an essential protein required for damage response and chromosome
484 segregation. Genetics 179: 757–771. https://doi.org/10.1534/genetics.107.085779
485 Green M. D. ., S. A. . Sabatinos, and S. L. . Forsburg, 2015 Microscopy Techniques to Examine DNA
486 Replication in Fission Yeast. Methods Mol Biol 1300: 13–41. https://doi.org/10.1016/B978-0-12-
487 374984-0.00431-9
488 Gursoy-Yuzugullu O., M. K. . Ayrapetov, and B. D. . Price, 2015 Histone chaperone Anp32e removes
489 H2A.Z from DNA double-strand breaks and promotes nucleosome reorganization and DNA repair.
490 Proc. Natl. Acad. Sci. 112: 7507–7512. https://doi.org/10.1073/pnas.1504868112
491 House N. C. M., J. H. Yang, S. C. Walsh, J. M. Moy, and C. H. Freudenreich, 2014 NuA4 Initiates Dynamic
492 Histone H4 Acetylation to Promote High-Fidelity Sister Chromatid Recombination at Postreplication

493 Gaps. Mol. Cell 55: 818–828. https://doi.org/10.1016/j.molcel.2014.07.007
494 Ikura T., S. Tashiro, A. Kakino, H. Shima, N. Jacob, *et al.*, 2007 DNA Damage-Dependent Acetylation and
495 Ubiquitination of H2AX Enhances Chromatin Dynamics. Mol. Cell. Biol. 27: 7028–7040.
496 https://doi.org/10.1128/MCB.00579-07
497 Jacquet K., A. Fradet-Turcotte, N. Avvakumov, J. P. Lambert, C. Roques, *et al.*, 2016 The TIP60 Complex
498 Regulates Bivalent Chromatin Recognition by 53BP1 through Direct H4K20me Binding and H2AK15
499 Acetylation. Mol. Cell 62: 409–421. https://doi.org/10.1016/j.molcel.2016.03.031
500 Javaheri A., R. Wysocki, O. Jobin-Robitaille, M. Altaf, J. Cote, *et al.*, 2006 Yeast G1 DNA damage
501 checkpoint regulation by H2A phosphorylation is independent of chromatin remodeling. Proc. Natl.
502 Acad. Sci. 103: 13771–13776. https://doi.org/10.1073/pnas.0511192103
503 Jha S., E. Shibata, and A. Dutta, 2008 Human Rvb1/Tip49 Is Required for the Histone Acetyltransferase
504 Activity of Tip60/NuA4 and for the Downregulation of Phosphorylation on H2AX after DNA Damage.
505 Mol. Cell. Biol. 28: 2690–2700. https://doi.org/10.1128/MCB.01983-07
506 Jiang X., Y. Sun, S. Chen, K. Roy, and B. D. Price, 2006 The FATC domains of PIKK proteins are
507 functionally equivalent and participate in the Tip60-dependent activation of DNA-PKcs and ATM. J.
508 Biol. Chem. 281: 15741–15746. https://doi.org/10.1074/jbc.M513172200
509 Jiang Y., X. Qian, J. Shen, Y. Wang, X. Li, *et al.*, 2015 Local generation of fumarate promotes DNA repair
510 through inhibition of histone H3 demethylation. Nat. Cell Biol. 17: 1158–1168.
511 https://doi.org/10.1038/ncb3209
512 Judes G., K. Rifaï, M. Ngollo, M. Daures, Y. J. Bignon, *et al.*, 2015 A bivalent role of TIP60 histone acetyl
513 transferase in human cancer. Epigenomics.
514 Kalocsay M., N. J. Hiller, and S. Jentsch, 2009 Chromosome-wide Rad51 Spreading and SUMO-H2A.Z-
515 Dependent Chromosome Fixation in Response to a Persistent DNA Double-Strand Break. Mol. Cell 33:
516 335–343. https://doi.org/10.1016/j.molcel.2009.01.016
517 Keogh M., T. A. Mennella, C. Sawa, S. Berthelet, N. J. Krogan, *et al.*, 2006 The Saccharomyces cerevisiae
518 histone H2A variant Htz1 is acetylated by NuA4. Genes Dev. 20: 660–665.
519 https://doi.org/10.1101/gad.1388106
520 Kim M.-Y., E.-J. Ann, J.-Y. Kim, J.-S. Mo, J.-H. Park, *et al.*, 2007 Tip60 Histone Acetyltransferase Acts as a
521 Negative Regulator of Notch1 Signaling by Means of Acetylation. Mol. Cell. Biol.
522 https://doi.org/10.1128/mcb.01515-06
523 Kim H. S., V. Vanoosthuyse, J. Fillingham, A. Roguev, S. Watt, *et al.*, 2009 An acetylated form of histone
524 H2A.Z regulates chromosome architecture in Schizosaccharomyces pombe. Nat. Struct. Mol. Biol. 16:
525 1286–1293. https://doi.org/10.1038/nsmb.1688

526 Kimura A., and M. Horikoshi, 1998 Tip60 acetylates six lysines of a specific class in core histones in vitro.
527 Genes to Cells 3: 789–800. https://doi.org/10.1046/j.1365-2443.1998.00229.x
528 Kobayashi J., A. Kato, Y. Ota, R. Ohba, and K. Komatsu, 2010 Bisbenzamidine derivative, pentamidine
529 represses DNA damage response through inhibition of histone H2A acetylation. Mol. Cancer 9: 1–11.
530 https://doi.org/10.1186/1476-4598-9-34
531 Kobor M. S., S. Venkatasubrahmanyam, M. D. Meneghini, J. W. Gin, J. L. Jennings, *et al.*, 2004 A Protein
532 Complex Containing the Conserved Swi2/Snf2-Related ATPase Swr1p Deposits Histone Variant
533 H2A.Z into Euchromatin. PLoS Biol. 2: 4. https://doi.org/10.1097/GME.0000000000000420
534 Krogan N. J. ., K. Baetz, M. Keogh, N. Datta, C. Sawa, *et al.*, 2004 Regulation of chromosome stability by
535 the histone H2A variant Htz1, the Swr1 chromatin remodeling complex, and the histone
536 acetyltransferase NuA4. Proc. Natl. Acad. Sci. 101: 13513–13518.
537 Kusch T., L. Florens, W. H. MacDonald, S. K. Swanson, R. L. Glaser, *et al.*, 2004 Acetylation by Tip60 is
538 required for selective histone variant exchange at DNA lesions. Science (80-.). 306: 2084–2087.
539 https://doi.org/10.1126/science.1103455
540 La Cruz X. De, S. Lois, S. Sánchez-Molina, and M. A. Martínez-Balbás, 2005 Do protein motifs read the
541 histone code? BioEssays.
542 Lafon A., C. S. Chang, E. M. Scott, S. J. Jacobson, and L. Pillus, 2007 MYST opportunities for growth
543 control: Yeast genes illuminate human cancer gene functions. Oncogene 26: 5373–5384.
544 https://doi.org/10.1038/sj.onc.1210606
545 Langerak P., E. Mejia-Ramirez, O. Limbo, and P. Russell, 2011 Release of Ku and MRN from DNA ends by
546 Mre11 nuclease activity and Ctp1 is required for homologous recombination repair of double-strand
547 breaks. PLoS Genet. 7. https://doi.org/10.1371/journal.pgen.1002271
548 Langerak P., and P. Russell, 2011 Regulatory networks integrating cell cycle control with DNA damage
549 checkpoints and double-strand break repair. Philos. Trans. R. Soc. B Biol. Sci. 366: 3562–3571.
550 https://doi.org/10.1098/rstb.2011.0070
551 Leduc C., P. Claverie, B. Eymin, E. Col, S. Khochbin, *et al.*, 2006 p14ARF promotes RB accumulation
552 through inhibition of its Tip60-dependent acetylation. Oncogene.
553 https://doi.org/10.1038/sj.onc.1209446
554 Leland B. A., A. C. Chen, A. Y. Zhao, R. C. Wharton, and M. C. King, 2018 Rev7 and 53BP1/CRB2
555 prevent RecQ helicase-dependent hyper-resection of DNA double-strand breaks. Elife 7: 1–14.
556 https://doi.org/10.7554/eLife.33402
557 Li L., and Y. Wang, 2017 Cross-talk between the H3K36me3 and H4K16ac histone epigenetic marks in
558 DNA double-strand break repair. J. Biol. Chem. 292: 11951–11959.

559 https://doi.org/10.1074/jbc.M117.788224
560 Manolis K. G., E. R. Nimmo, E. Hartsuiker, A. M. Carr, P. A. Jeggo, *et al.*, 2001 Novel functional
561 requirements for non-homologous DNA end joining in Schizosaccharomyces pombe. EMBO J. 20:
562 210–221. https://doi.org/10.1093/emboj/20.1.210
563 Millar C. B. ., F. Xu, K. Zhang, and M. Grunstein, 2006 Acetylation of H2AZ Lys 14 is associated with
564 genome-wide gene activity in yeast. Genes Dev. 20: 711–722. https://doi.org/10.1101/gad.1395506
565 Minoda A., S. Saitoh, K. Takahashi, and T. Toda, 2005 BAF53/Arp4 Homolog Alp5 in Fission Yeast Is
566 Required for Histone H4 Acetylation, Kinetochore-Spindle Attachment, and Gene Silencing at
567 Centromere. Mol. Biol. Cell 16: 316–327. https://doi.org/10.1091/mbc.E04
568 Miyoshi T., J. Kanoh, and F. Ishikawa, 2009 Fission yeast Ku protein is required for recovery from DNA
569 replication stress. Genes to Cells. https://doi.org/10.1111/j.1365-2443.2009.01337.x
570 Morillo-huesca M., M. Clemente-ruiz, E. Andujar, and F. Prado, 2010 The SWR1 Histone Replacement
571 Complex Causes Genetic Instability and Genome-Wide Transcription Misregulation in the Absence of
572 H2A . Z. PLoS One 5. https://doi.org/10.1371/journal.pone.0012143
573 Morishita T., Y. Tsutsui, H. Iwasaki, and H. Shinagawa, 2003 The Schizosaccharomyces pombe rad60 Gene
574 Is Essential for Repairing Double-Strand DNA Breaks Spontaneously Occurring during Replication and
575 Induced by DNA-Damaging Agents. Mol. Cell. Biol. 23: 3373–3373.
576 https://doi.org/10.1128/mcb.23.9.3373.2003
577 Murr R., J. I. Loizou, Y. G. Yang, C. Cuenin, H. Li, *et al.*, 2005 Histone acetylation by Trrap-Tip60
578 modulates loading of repair proteins and repair of DNA double-strand breaks. Nat. Cell Biol. 8: 91–99.
579 https://doi.org/10.1038/ncb1343
580 Myler L. R., I. F. Gallardo, M. M. Soniat, A. Rajashree, X. B. Gonzalez, *et al.*, 2017 Single-molecule
581 imaging reveals how Mre11-Rad50-Nbs1 initiates DNA break repair. Mol. Cell 67: 891–898.
582 https://doi.org/10.1016/j.molcel.2017.08.002.Single-molecule
583 Naidu S. R., A. J. Lakhter, and E. J. Androphy, 2012 PIASy-mediated Tip60 sumoylation regulates p53-
584 induced autophagy. Cell Cycle 11: 2717–2728. https://doi.org/10.4161/cc.21091
585 Noguchi C., T. Singh, M. A. Ziegler, J. D. Peake, L. Khair, *et al.*, 2019 The NuA4 acetyltransferase and
586 histone H4 acetylation promote replication recovery after topoisomerase I-poisoning. Epigenetics and
587 Chromatin 12: 1–17. https://doi.org/10.1186/s13072-019-0271-z
588 Nugent R. L., A. Johnsson, B. Fleharty, M. Gogol, Y. Xue-Franzén, *et al.*, 2010 Expression profiling of S.
589 pombe acetyltransferase mutants identifies redundant pathways of gene regulation. BMC Genomics 11.
590 https://doi.org/10.1186/1471-2164-11-59
591 Onaka A. T., N. Toyofuku, T. Inoue, A. K. Okita, M. Sagawa, *et al.*, 2016 Rad51 and Rad54 promote

592 noncrossover recombination between centromere repeats on the same chromatid to prevent
593 isochromosome formation. Nucleic Acids Res. 44: 10744–10757. https://doi.org/10.1093/nar/gkw874
594 Ortega-Atienza S., V. C. Wong, Z. DeLoughery, M. W. Luczak, and A. Zhitkovich, 2016 ATM and KAT5
595 safeguard replicating chromatin against formaldehyde damage. Nucleic Acids Res. 44: 198–209.
596 https://doi.org/10.1093/nar/gkv957
597 Osman F., E. A. Fortunato, and S. Subramani, 1996 Double-strand break-induced mitotic intrachromosomal
598 recombination in the fission yeast Schizosaccharomyces pombe. Genetics 142: 341–357.
599 Osman F., M. Adriance, and S. McCready, 2000 The genetic control of spontaneous and UV-induced mitotic
600 intrachromosomal recombination in the fission yeast Schizosaccharomyces pombe. Curr. Genet. 38:
601 113–125. https://doi.org/10.1007/s002940000145
602 Papamichos-Chronakis M., S. Watanabe, O. J. Rando, and C. L. Peterson, 2011 Global regulation of H2A.Z
603 localization by the INO80 chromatin-remodeling enzyme is essential for genome integrity. Cell 144:
604 200–213. https://doi.org/10.1016/j.cell.2010.12.021
605 Pillus L., 2008 MYSTs mark chromatin for chromosomal functions. Curr. Opin. Cell Biol. 20: 326–333.
606 https://doi.org/10.1016/j.ceb.2008.04.009
607 Prudden J., J. S. Evans, S. P. Hussey, B. Deans, P. O'Neill, *et al.*, 2003 Pathway utilization in response to a
608 site-specific DNA double-strand break in fission yeast. EMBO J. https://doi.org/10.1093/emboj/cdg119
609 Renaud-Young M., D. C. Lloyd, K. Chatfield-Reed, I. George, G. Chua, *et al.*, 2015 The NuA4 complex
610 promotes translesion synthesis (TLS)-mediated DNA damage tolerance. Genetics 199: 1065–1076.
611 https://doi.org/10.1534/genetics.115.174490
612 Renaud E., A. Barascu, and F. Rosselli, 2015 Impaired TIP60-mediated H4K16 acetylation accounts for the
613 aberrant chromatin accumulation of 53BP1 and RAP80 in Fanconi anemia pathway-deficient cells.
614 Nucleic Acids Res. 44: 648–656. https://doi.org/10.1093/nar/gkv1019
615 Sabatinos S. A., and S. L. Forsburg, 2010 Molecular genetics of schizosaccharomyces pombe. Methods
616 Enzymol. 470: 759–795. https://doi.org/10.1016/S0076-6879(10)70032-X
617 Sánchez A., and P. Russell, 2015 Ku Stabilizes replication forks in the absence of Brc1. PLoS One.
618 https://doi.org/10.1371/journal.pone.0126598
619 Sapountzi V., I. R. Logan, and C. N. Robson, 2006 Cellular functions of TIP60. Int. J. Biochem. Cell Biol.
620 38: 1496–1509. https://doi.org/10.1016/j.biocel.2006.03.003
621 Scacchetti A., and P. B. Becker, 2021 Variation on a theme: Evolutionary strategies for H2A.Z exchange by
622 SWR1-type remodelers. Curr. Opin. Cell Biol.
623 Schindelin J., I. Arganda-Carreras, E. Frise, V. Kaynig, M. Longair, *et al.*, 2012 Fiji: An open-source
624 platform for biological-image analysis. Nat. Methods.

625 Schuchert P., and J. Kohli, 1988 The ade6-M26 Mutation of Schizosaccharomyces pombe Increases the
626 Frequency of Crossing Over. Genetics 119: 507–515.
627 Semer M., B. Bidon, A. Larnicol, G. Caliskan, P. Catez, *et al.*, 2019 DNA repair complex licenses
628 acetylation of H2A.Z.1 by KAT2A during transcription. Nat. Chem. Biol. 15: 992–1000.
629 https://doi.org/10.1038/s41589-019-0354-y
630 Shao Z., A. J. Davis, K. R. Fattah, S. So, J. Sun, *et al.*, 2012 Persistently bound Ku at DNA ends attenuates
631 DNA end resection and homologous recombination. DNA Repair (Amst). 11: 310–316.
632 https://doi.org/10.1016/j.dnarep.2011.12.007
633 Sharma G. G., S. So, A. Gupta, R. Kumar, C. Cayrou, *et al.*, 2010 MOF and Histone H4 Acetylation at
634 Lysine 16 Are Critical for DNA Damage Response and Double-Strand Break Repair. Mol. Cell. Biol.
635 30: 3582–3595. https://doi.org/10.1128/mcb.01476-09
636 Shastri N., Y. C. Tsai, S. Hile, D. Jordan, B. Powell, *et al.*, 2018 Genome-wide Identification of Structure-
637 Forming Repeats as Principal Sites of Fork Collapse upon ATR Inhibition. Mol. Cell 72: 222-238.e11.
638 https://doi.org/10.1016/j.molcel.2018.08.047
639 Shibata A., P. Jeggo, and M. Löbrich, 2018 The pendulum of the Ku-Ku clock. DNA Repair (Amst). 71:
640 164–171. https://doi.org/10.1016/j.dnarep.2018.08.020
641 Smith E. R., A. Eisen, W. Gu, M. Sattah, A. Pannuti, *et al.*, 1998 ESA1 is a histone acetyltransferase that is
642 essential for growth in yeast. Proc Natl Acad Sci USA 95: 3561–3565.
643 https://doi.org/10.1073/pnas.95.7.3561
644 Soria G., S. E. Polo, and G. Almouzni, 2012 Prime, Repair, Restore: The Active Role of Chromatin in the
645 DNA Damage Response. Mol. Cell 46: 722–734. https://doi.org/10.1016/j.molcel.2012.06.002
646 Stubbe J., and J. W. Kozarich, 1987 Mechanisms of Bleomycin-Induced DNA Degradation. Chem. Rev. 87:
647 1107–1136. https://doi.org/10.1021/cr00081a011
648 Sun Y., X. Jiang, S. Chen, N. Fernandes, and B. D. Price, 2005 A role for the Tip60 histone acetyltransferase
649 in the acetylation and activation of ATM. Proc. Natl. Acad. Sci. U. S. A. 102: 13182–13187.
650 https://doi.org/10.1073/pnas.0504211102
651 Sun Y., X. Jiang, Y. Xu, M. K. Ayrapetov, L. A. Moreau, *et al.*, 2009 Histone H3 methylation links DNA
652 damage detection to activation of the tumour suppressor Tip60. Nat. Cell Biol. 11: 1376–1382.
653 https://doi.org/10.1038/ncb1982
654 Syed A., and J. A. Tainer, 2018 The MRE11–RAD50–NBS1 Complex Conducts the Orchestration of
655 Damage Signaling and Outcomes to Stress in DNA Replication and Repair. Annu. Rev. Biochem. 87:
656 263–294. https://doi.org/10.1146/annurev-biochem-062917-012415
657 Sykes S. M., H. S. Mellert, M. A. Holbert, K. Li, R. Marmorstein, *et al.*, 2006 Acetylation of the p53 DNA-

658 Binding Domain Regulates Apoptosis Induction. Mol. Cell 24: 841–851.
659 https://doi.org/10.1016/j.molcel.2006.11.026
660 Tang Y., J. Luo, W. Zhang, and W. Gu, 2006 Tip60-Dependent Acetylation of p53 Modulates the Decision
661 between Cell-Cycle Arrest and Apoptosis. Mol. Cell 24: 827–839.
662 https://doi.org/10.1016/j.molcel.2006.11.021
663 Tang J., N. W. Cho, G. Cui, E. M. Manion, N. M. Shanbhag, *et al.*, 2013 Acetylation limits 53BP1
664 association with damaged chromatin to promote homologous recombination. Nat. Struct. Mol. Biol. 20:
665 317–325. https://doi.org/10.1038/nsmb.2499
666 Teixeira-Silva A., A. Ait Saada, J. Hardy, I. Iraqui, M. C. Nocente, *et al.*, 2017 The end-joining factor Ku
667 acts in the end-resection of double strand break-free arrested replication forks. Nat. Commun. 8.
668 https://doi.org/10.1038/s41467-017-02144-5
669 Thomas T., and A. K. Voss, 2007 The diverse biological roles of MYST histone acetyltransferase family
670 proteins. Cell Cycle.
671 Tomita K., A. Matsuura, T. Caspari, A. M. Carr, Y. Akamatsu, *et al.*, 2003 Competition between the Rad50
672 Complex and the Ku Heterodimer Reveals a Role for Exol in Processing Double-Strand Break. Mol.
673 Cell. Biol. 23: 5186–5197. https://doi.org/10.1128/MCB.23.15.5186
674 Utley R. T., and J. Côté, 2003 The MYST family of histone acetyltransferases. Curr. Top. Microbiol.
675 Immunol.
676 Van H. T., and M. A. Santos, 2018 Histone modifications and the DNA double-strand break response. Cell
677 Cycle.
678 Voss A. K., and T. Thomas, 2009 MYST family histone acetyltransferases take center stage in stem cells and
679 development. BioEssays.
680 Walworth N. C., and R. Bernards, 1996 rad-Dependent Response of the chk1-Encoded Protein Kinase at the
681 DNA Damage Checkpoint. Science (80-.). 271: 353–356.
682 Wan S., H. Capasso, and N. C. Walworth, 1999 The topoisomerase I poison camptothecin generates a Chk1-
683 dependent DNA damage checkpoint signal in fission yeast. Yeast 15: 821–828.
684 https://doi.org/10.1002/(SICI)1097-0061(199907)15:10A<821::AID-YEA422>3.0.CO;2-#
685 Wang H., and X. Xu, 2017 Microhomology-mediated end joining: New players join the team. Cell Biosci. 7:
686 4–9. https://doi.org/10.1186/s13578-017-0136-8
687 Xhemalce B., and T. Kouzarides, 2010 A chromodomain switch mediated by histone H3 Lys 4 acetylation
688 regulates heterochromatin assembly. Genes Dev. 24: 647–652. https://doi.org/10.1101/gad.1881710
689 Xu Y., Y. Sun, X. Jiang, M. K. Ayrapetov, P. Moskwa, *et al.*, 2010 The p400 ATPase regulates nucleosome
690 stability and chromatin ubiquitination during DNA repair. J. Cell Biol. 191: 31–43.

691 https://doi.org/10.1083/jcb.201001160
692 Xu Y., M. K. Ayrapetov, C. Xu, O. Gursoy-Yuzugullu, Y. Hu, *et al.*, 2012 Histone H2A.Z Controls a
693 Critical Chromatin Remodeling Step Required for DNA Double-Strand Break Repair. Mol. Cell 48:
694 723–733. https://doi.org/10.1016/j.molcel.2012.09.026
695 Yan Z., C. Xue, S. Kumar, J. B. Crickard, Y. Yu, *et al.*, 2019 Rad52 Restrains Resection at DNA Double-
696 Strand Break Ends in Yeast. Mol. Cell 76: 699-711.e6. https://doi.org/10.1016/j.molcel.2019.08.017
697 Yu Y., J. Y. Ren, J. M. Zhang, F. Suo, X. F. Fang, *et al.*, 2013 A proteome-wide visual screen identifies
698 fission yeast proteins localizing to DNA double-strand breaks. DNA Repair (Amst). 12: 433–443.
699 https://doi.org/10.1016/j.dnarep.2013.04.001
700 Zhou B. O., S. S. Wang, L. X. Xu, F. L. Meng, Y. J. Xuan, *et al.*, 2010 SWR1 Complex Poises
701 Heterochromatin Boundaries for Antisilencing Activity Propagation. Mol. Cell. Biol. 30: 2391–2400.
702 https://doi.org/10.1128/MCB.01106-09
703 Zhu Z., W. H. Chung, E. Y. Shim, S. E. Lee, and G. Ira, 2008 Sgs1 Helicase and Two Nucleases Dna2 and
704 Exo1 Resect DNA Double-Strand Break Ends. Cell 134: 981–994.
705 https://doi.org/10.1016/j.cell.2008.08.037
706 Zlatanova J., and A. Thakar, 2008 H2A.Z: View from the Top. Structure 16: 166–179.
707 https://doi.org/10.1016/j.str.2007.12.008
708

709 **Figure Legends**

710 **Figure 1. The *mst1-L344S* allele affects DSB repair. A.** *mst1-L344S* are sensitive to bleomycin. Cells were
711 grown in YES media overnight at 25ºC then 5X serial dilutions were spotted onto YES plates or YES plates
712 containing bleomycin. Plates were incubated at 25ºC and photographed after 4 days. 1 unit of bleomycin = 1
713 mg (by potency). **B.** An assay to test chromosomal instability from (Osman *et al.* 1996). Two non-functional
714 *ade6* alleles flank the functional *ura4*$^{+}$ gene. *the ade6-L469* has a mutation at the C terminus while the *ade6-*
715 *M26* allele has a mutation at the N-terminus (indicated by the vertical lines). Several recombination outcomes
716 are possible and are described in results and methods. **C.** Cells were grown in YES media overnight at 25ºC
717 then 5X serial dilutions were spotted onto YES (*HO* repressed) or PMG without thiamine (*HO* induced). Plates
718 were incubated at 25ºC and photographed after 5 days. **D**. Percent of deletion, conversion and complex
719 rearrangements after double strand break induction in WT and *mst1-L344S* using the assay in **B**. The bold line
720 in each box represents median and the filled circles represent outliers. Asterisks indicate that recombination
721 percentage is significantly different than WT ($p<0.05$, Mann-Whitney Test). **E**. Chromatin
722 immunoprecipitation assay to test recruitment of Rad52-YFP and Mst1-V5 to a single DNA double strand
723 break in WT and *clr4*Δ. Using a construct from Du, Nakamura, and Russell 2006 with one single double strand
724 break can be made with the *HO* endonuclease and protein interaction with chromatin can be monitored at 0.2
725 and 2KB from the break. Following break induction, time points were taken at 0, 22, 24 and 26 hours. qPCR
726 was done with primers provided in Du, Nakamura, and Russell 2006. Asterisks represent fold enrichment is
727 significantly different than that in WT ($p<0.1$, Student's t-test).

728 **Figure 2. The *mst1-L344S* mutant affects recruitment of repair proteins at 25ºC A. Top:** Percentage of
729 cells with RPA (Rad11) and Rad52 foci in WT, *mst1-L344S*, *pht1-4KR*, *pht1*Δ, *ku70*Δ and *ku70*Δ *mst1-L344S.*
730 The bold line in each box represents median and the filled circles represent outliers. Asterisks represent
731 percentage of cells with foci is significantly different than that in WT (*: $p<0.05$, **: $p<0.01$, Mann-Whitney
732 Test) **Bottom:** Examples of WT and *mst1-L344S* cells with Rad11 and Rad52 foci. Scale bar is 10µm. Rad11-
733 CFP is colored magenta for visibility. **B. Top:** Percentage of cells with Rad54 foci in WT and *mst1-L344S,*
734 *pku70*Δ *and pku70*Δ *mst1-L344S.* The bold line in each box represents median and the filled circles represent
735 outliers. **Bottom:** Examples of WT and *mst1-L344S* cells with Rad54 foci under phleomycin treatment. Scale
736 bar is 10µm. **C. Top:** Percentage of cells with colocalized Rad52-CFP and HO-induced mCherry foci over
737 240 minutes. **Bottom:** Representatives of WT and *mst1-L344S* cells with Rad52-CFP and HO-induced
738 mCherry foci over time. Rad52-CFP is colored green for visibility. **D.** Percentage of cells with mCherry-LacI
739 signal over 240 minutes. Image was taken every 8 min in wild-type and *mst1-L344S*, and every 48 min in other
740 mutants.

741 **Figure 3. *mst1-L344S* mutants are sensitive to the DSB-inducing agent bleomycin.** *pku70*Δ, *exo1*Δ **(A.)**
742 and *pht1-4KR* **(B.)** growth in bleomycin. Cells were grown in YES media overnight at 25ºC then 5X serial
743 dilutions were spotted onto YES plates or YES plates containing bleomycin. Plates were incubated at 25ºC
744 and photographed after 4 days. 1 unit of bleomycin = 1 mg (by potency)
745 **Figure 4. Mst1 affects DNA lesion repair but does not affect checkpoint activation. A. Left:** Percentage
746 of cells with RPA (Rad11) and Rad52 foci in WT and *mst1-L344S* after CPT and MMS treatments. The bold
747 line in each box represents median and the filled circles represent outliers. **Right:** examples of WT and *mst1-*
748 *L344S* cells with RPA and Rad52 foci after drug treatment. Scale bar is 10µm. Rad11-CFP is colored magenta
749 for visibility. **B**. Phosphorylation of Chk1-HA is not affected in *mst1-L344S* after treatment of cells with three
750 types of DNA damaging agents at 32°C. cells were treated for 4 hours with 0.01% MMS, 15mM HU or 40µM
751 CPT and the and the Chk1-HA phosphorylation shift band was detected by Western blotting with 12CA5 anti-
752 HA antibody. **C**. H2A phosphorylation dynamics are not affected in *mst1-L344S* when cells are treated with
753 40µM CPT. Western Blot with an anti-phosphorylated H2A antibody showing that phosphorylation of H2A
754 peaks 4 hours after treatment with drug then the signal is down regulated 4 hours post drug removal. *hta1-*
755 *S129A:* control non-phosphorylatable form of H2A; α-PCNA: control antibody.
756 **Figure 5. Model for the function of Mst1 in DSB repair.** Mst1 facilitates HR by promoting long-range
757 resection and inhibiting Ku70-associated mechanism that inhibits HR. Such function is accomplished by
758 acetylating H2A.Z and thus promoting the turnover of H2A.Z at the DSB. Therefore, the histone variant can
759 no longer block the break site. The removal of H2A.Z allows Exo1 to access the break and thus promotes
760 downstream recombination-mediated repair.
761 **Supplementary Figure S1. *clr4*Δ had lower percentage of cells with Rad52 foci after single DSB**
762 **induction. Top:** Percentage of cells with Rad52 foci using a construct from Du, Nakamura, and Russell 2006
763 with one single double strand break can be made with the *HO* endonuclease. Following break induction,
764 cultures were taken at 0, 22, 24 and 26 hours as in Figure 1E and cells were imaged under microscope. Asterisks
765 represent fold enrichment is significantly different than that in WT ($p<0.05$, Student's t-test). **Bottom:**
766 Examples of WT and *clr4*Δ cells with Rad52 foci upon DSB induction.
767 **Supplementary Figure S2. *mst1-L344S* mutants are sensitive to Bleomycin analog Phleomycin.** Cells
768 were grown in YES media overnight at 25ºC then 5X serial dilutions were spotted onto YES plate or YES
769 plates containing Phleomycin. Plates were incubated at 25ºC and photographed after 4 days.
770 **Supplementary Figure S3**. **Examples of cells with RPA (Rad11), Rad52, and Rad54 foci after treatment**
771 **with phleomycin at 25ºC**. **A.** Rad11-CFP and Rad52-YFP foci in *pku70Δ* and *pku70Δ mst1-L344S*. **B.** Rad11-
772 CFP and Rad52-YFP foci in *pht1-4KR* and *pht1Δ*. **C.** Rad54-GFP foci in *pku70Δ* and *pku70Δ mst1-L344S.*

773 **Supplementary Figure S4. *pku70*Δ does not affect cell length at septation in *mst1-L344S* at 25ºC.** Length
774 at septation at 25ºC of WT, *mst1-L344S*, *pku70*Δ, and *pku70*Δ *mst1-L334S* cells. The bold line in each box
775 represents median and the filled circles represent outliers.
776 **Supplementary Figure S5. *mst1-L344S* interacts genetically with genes in the checkpoint pathways.** Cells
777 were grown in YES media overnight at 32ºC then 5X serial dilutions were spotted onto YES plate or YES
778 plates containing the indicated drugs. Plates were incubated at 32ºC and photographed after 4 days.
779 **Supplementary Table S1.** Median, first and third quantiles of cells with Rad11, Rad52 or Rad54 percentage
780 shown in Figure 2A and 2B.
781 **Supplementary Table S2.** Strains used in this study.
782

Figure 1. The *mst1-L344S* allele affects DSB repair.

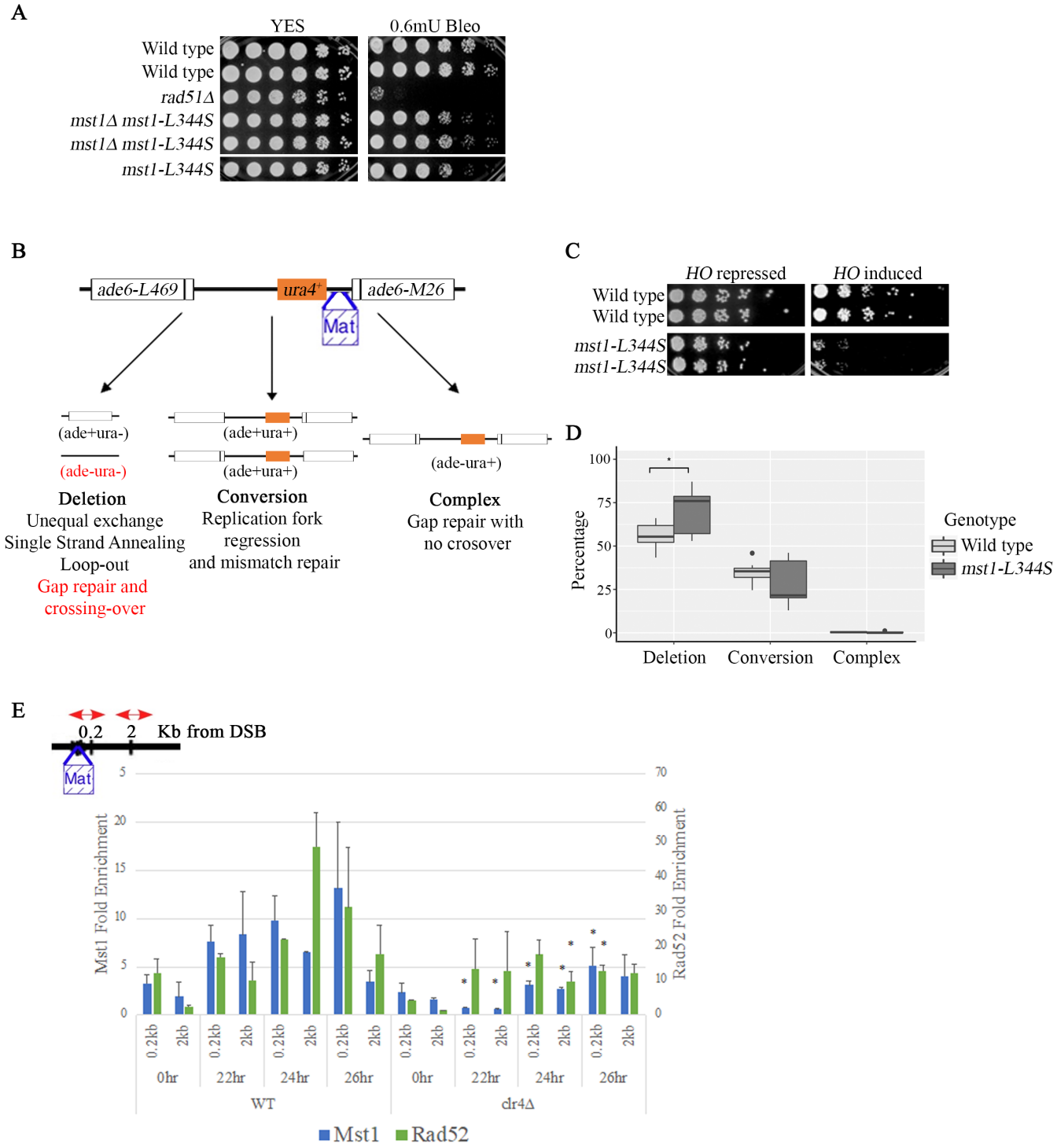

783

Figure 2. The *mst1-L344S* mutant affects recruitment of repair proteins.

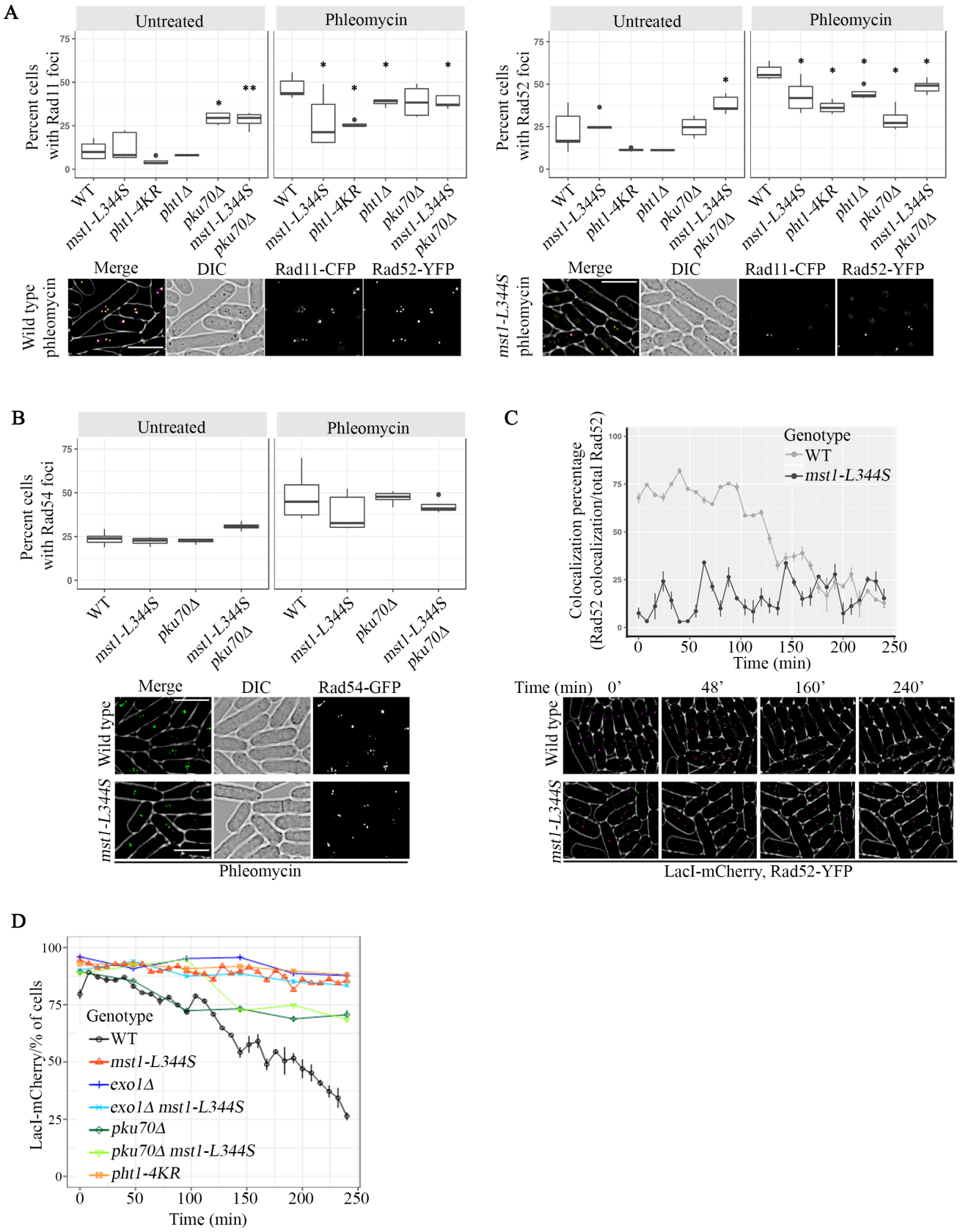

Figure 3. *mst1-L344S* mutants are sensitive to the DSB-inducing agent bleomycin.

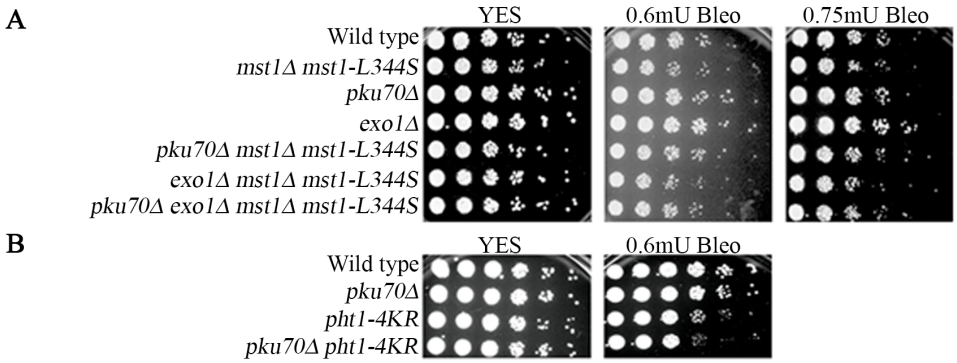

785

Figure 4. Mst1 affects DNA lesion repair but does not affect checkpoint activation.

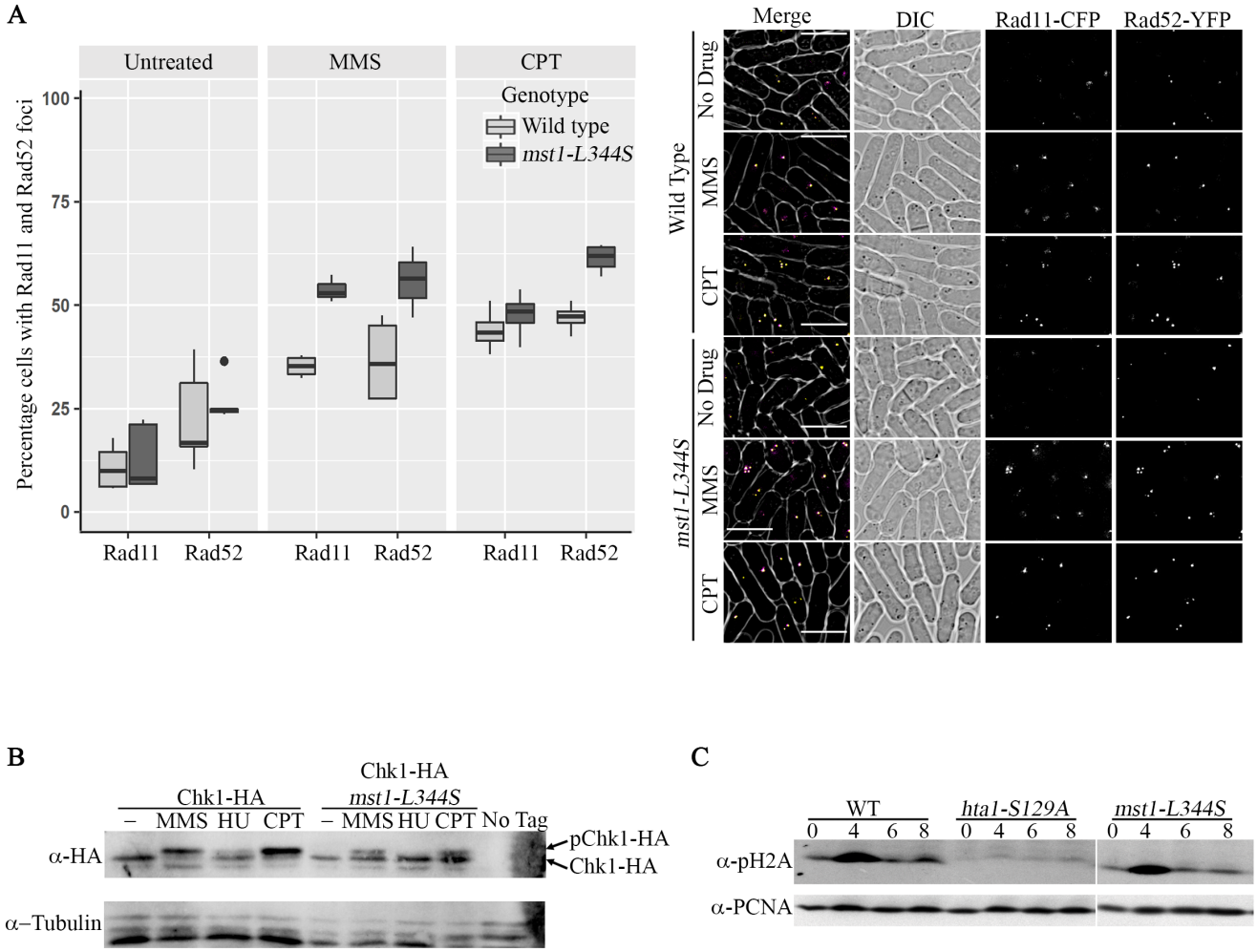

786

Figure 5. Model for the function of Mst1

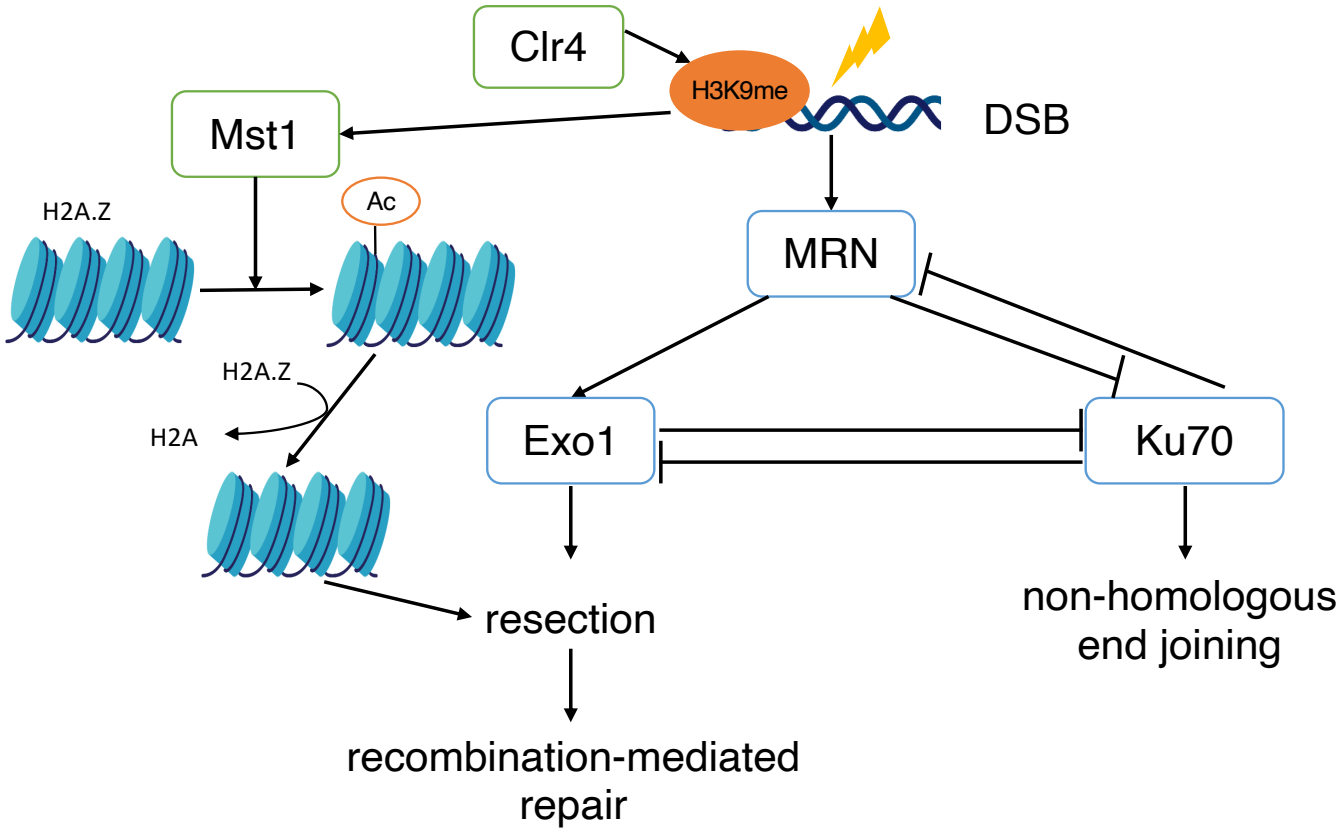

787

Supplementary Figure S1. Decreased levels of RAD52-YFP foci in *clr4Δ* compared to WT follwoing induction of a single DSB.

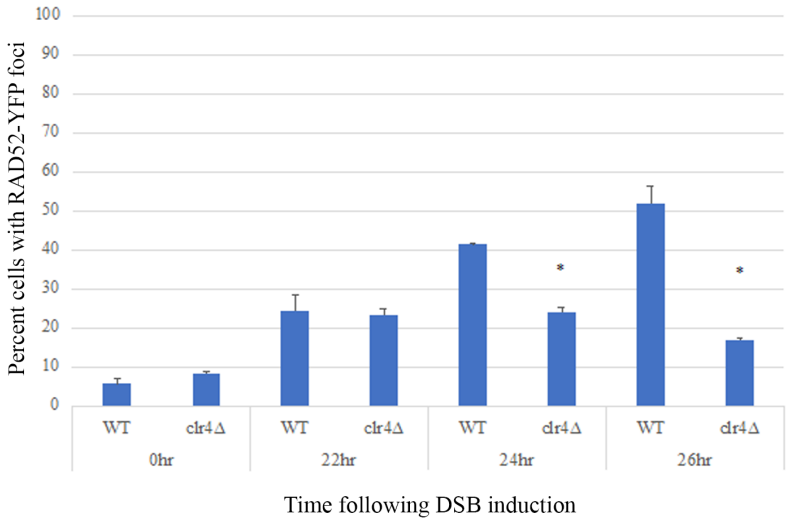

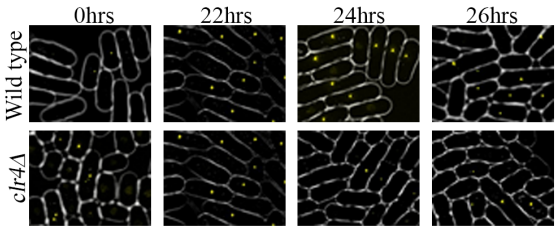

788

Supplementary Figure S2. The *mst1-L344S* mutants are sensitive to the bleomycin analog phelomycin.

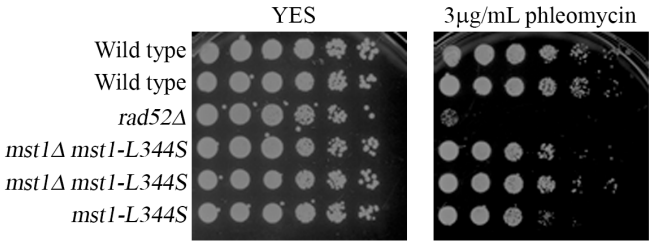

789

Supplementary Figure S3. Examples of cell with RPA (Rad11), Rad52, and Rad54 foci after treatement with phleomycin.

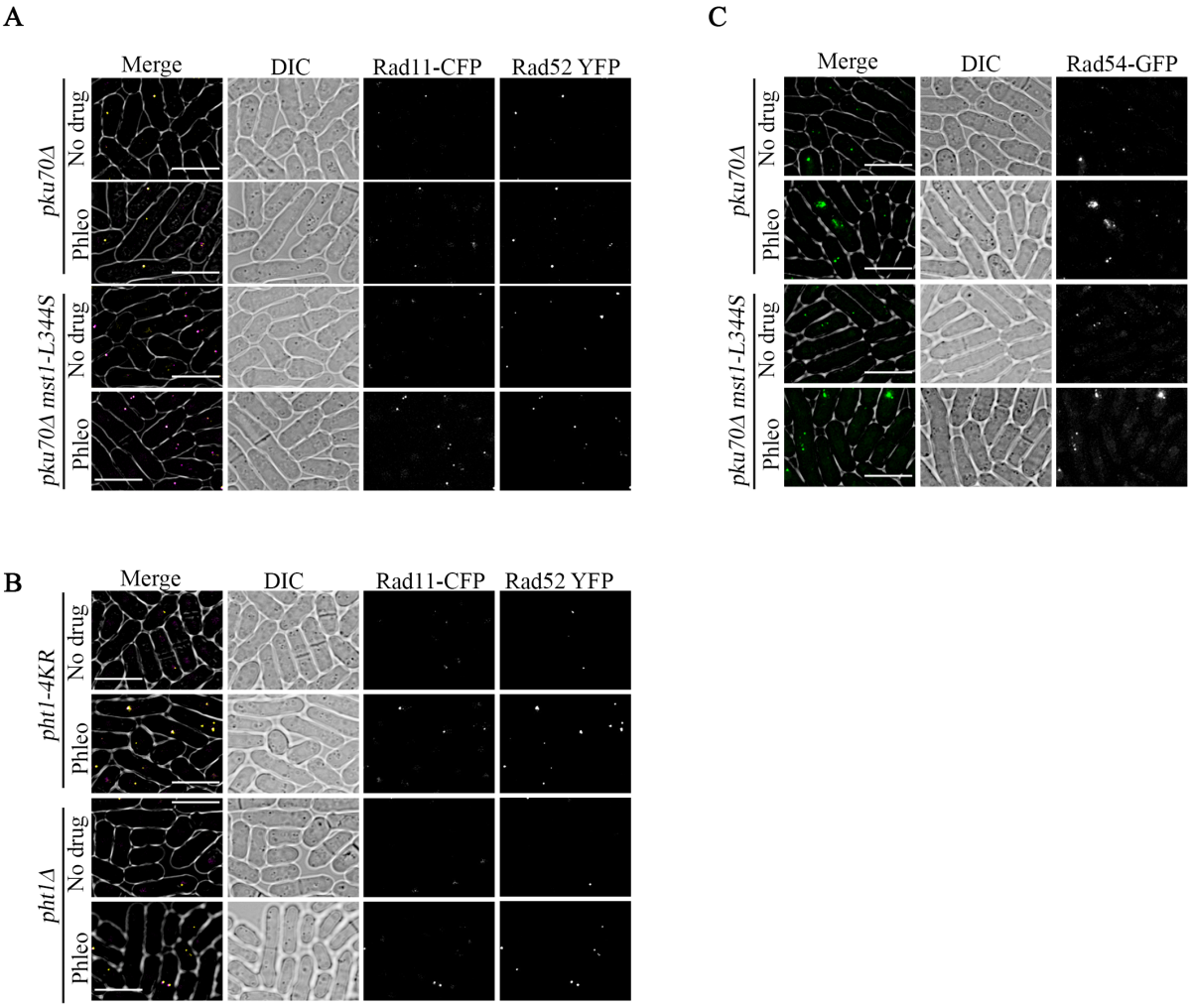

Supplementary Figure S4. ***pku70Δ*** does not affect cell length at septation in ***mst1-L344S*** at 25°C.

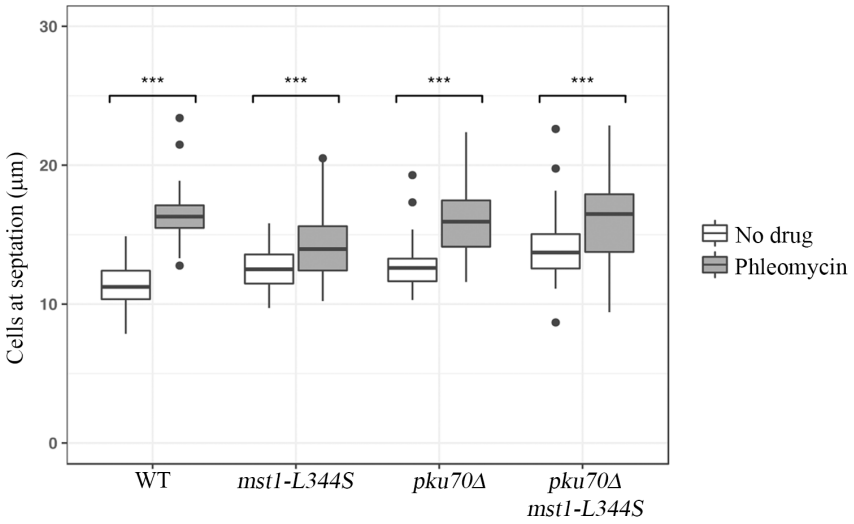

Supplementary Figure S5. ***mst1-L344S*** interacts genetically with genes in the checkpoint pathways.

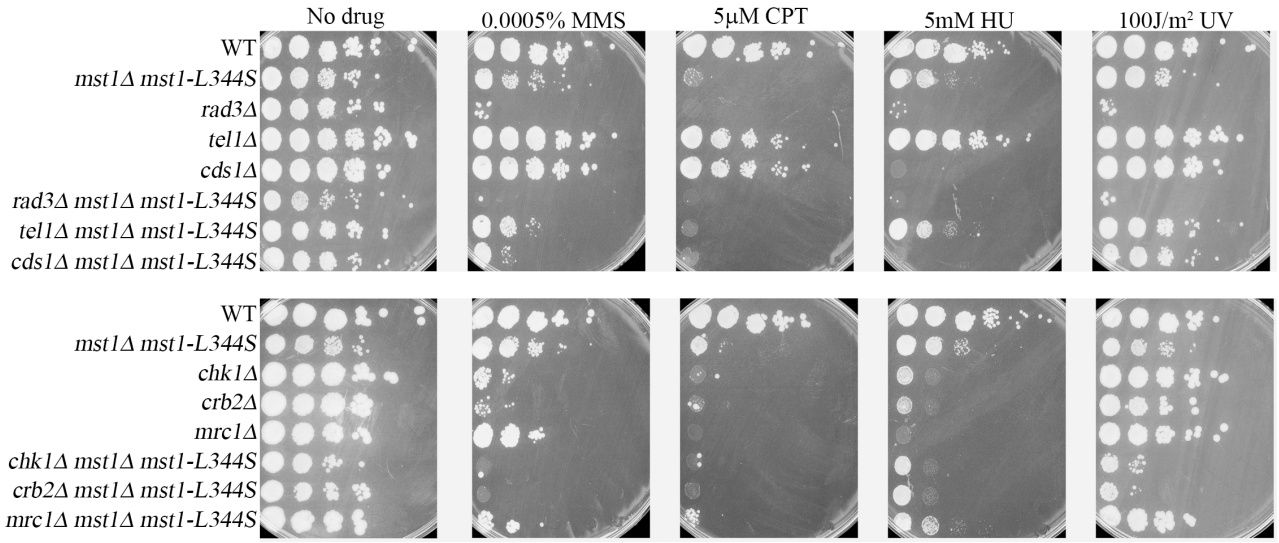

792

Supplementary Table S1. Median, first and third quartiles of cells with Rad11-CFP, Rad52-YFP and Rad54-GFP foci percentages.

	Rad11		
	Median	1st Quantile	3rd Quantile
WT Untreated	9.9	6.1	14.51
WT Phleomycin	43.72	42.98	50.7
mst1-L344S Untreated	8.14	6.76	21.15
mst1-L344S Phleomycin	21.3	15.38	37.29
pht1-4KR Untreated	3.58	3.25	4.78
pht1-4KR Phleomycin	24.96	24.76	25.95
*pht1*Δ Untreated	7.99	7.7	8.36
*pht1*Δ Phleomycin	39.2	37.75	39.86
*pku70*Δ Untreated	29.48	26.4	32.27
*pku70*Δ Phleomycin	38.31	30.99	46.27
*pku70*Δ *mst1-L344S* Untreated	29.5	26.38	31.32
*pku70*Δ *mst1-L344S* Phleomycin	37.08	36.62	42.3

	Rad52		
	Median	1st Quantile	3rd Quantile
WT Untreated	16.67	15.85	31.17
WT Phleomycin	55.4	53.77	60
mst1-L344S Untreated	24.73	24.12	24.89
mst1-L344S Phleomycin	41.85	35.76	24.89
pht1-4KR Untreated	11.26	10.98	11.63
pht1-4KR Phleomycin	36.05	33.84	38.7
*pht1*Δ Untreated	11.11	11.11	11.51
*pht1*Δ Phleomycin	43.42	42.53	45.59
*pku70*Δ Untreated	24.7	20.28	29.16
*pku70*Δ Phleomycin	27.19	24.71	31.83
*pku70*Δ *mst1-L344S* Untreated	35.75	35.2	42.32
*pku70*Δ *mst1-L344S* Phleomycin	49.09	46.02	50.4

	Rad54		
	Median	1st Quantile	3rd Quantile
WT Untreated	23.91	21.72	25.22
WT Phleomycin	44.91	37.34	54.55
mst1-L344S Untreated	22.74	21.18	23.85
mst1-L344S Phleomycin	32.7	30.28	47.48
*pku70*Δ Untreated	23.04	22.06	23.47
*pku70*Δ Phleomycin	47.78	46.09	49.55
*pku70*Δ *mst1-L344S* Untreated	30.74	29.99	31.6
*pku70*Δ *mst1-L344S* Phleomycin	40.97	40.04	43.37

793

794 **Supplementary Table S2.** Strains used in this study.
795

Strain	Genotype	Source
FY254	*h- can1-1 leu1-32 ade6-M210 ura4-D18*	Our stock
FY255	*h+ can1-1 leu1-32 ade6-M210 ura4-D18*	Our stock
FY527	*h- his3-D1 ade6-M216 ura4-D18 leu1-32*	Our stock
FY528	*h+ his3-D1 ade6-M210 ura4-D18 leu1-32*	Our stock
FY421	*h- ade6-704 leu1-32 ura4-D18 Δchk1::ura4*	Our stock
FY4743	*h- rad11-Cerulean::hphMX rad22-YFP-natMX leu1-32 ade6-M210 ura4-D18*	Our stock
FY8927	*h90 mst1-L344S-5FLAG:hphMX6 rad11-Cerulean::hphMX rad22-YFP-natMX leu1-32 ura4-D18*	This study
FY1106	*h+ Δrad3::ura4+ ura4-D18 leu1-32 ade6-M210*	Our stock
FY1204	*h+ Δrhp51::ura4+ ade6-704 leu1-32 ura4-D18*	Our stock
FY1353	*h+ leu1-32 ura4-D18 his3-D1 ade6-M210 pku70::kanr*	Our stock
FY2396	*h- Δmst1::ura4+ leu1::nmt-mst1L-S leu1+ ura4-D18 ade6-M210*	Our stock
FY2449	*h+ Δmst1::kanMX6 leu1::nmt-mst1L-S-leu1+ ura4-D18 ade6-M210*	Our stock
FY2450	*h- Δmst1::kanMX6 leu1::nmt-mst1L-S-leu1+ ura4-D18 ade6-M210*	Our stock
FY2504	*h- Δrhp9::ura4+ (=crb2) mst1::kanMX6 leu1::nmt-mst1L-S-leu1+ ura4-D18 leu1-32 ade6-M21?*	This study
FY2643	*h- Δchk1::ura4+ Δmst1::kanMX6 leu1::nmt-mst1L-S-leu1+ ura4-D18 ade6-M210 or 704*	Our stock
FY2725	*h- Δpku70::kanr Δmst1::ura4+ leu1::nmt-mst1L-S leu1+ ura4-D18 ade6-M210*	Our stock
FY2726	*h- Δpku70::kanr Δmst1::ura4+ leu1::nmt-mst1L-S leu1+ ura4-D18 ade6-M210*	Our stock
FY3135	*h- ade6-M210 leu1-32 ura4-D18 hip1::ura4+*	Simon Whitehall
FY3151	*h- Δmrc1::ura4+ ura4-D18 leu1-32 his7-366*	Our stock
FY3439	*h- ura4-D18 leu1-32 ade6-M216 his3-D1 Δrhp9::ura4+ (=crb2)*	Our stock
FY3562	*h+ Δmst1::kanMX6 leu1::nmt-mst1L-S-leu1+ ade6-M210 ura4-D18 Δhip1::ura4+*	Our stock
FY3857	*h+ Δrhp51::ura4+ Δmst1::kanMX6 leu1::nmt-mst1L-S leu1+ura4-D18 leu1-32*	This study
FY3884	*h- exo1::ura4 ura4-D18*	Mathew O'Connell
FY4713	*h- Δmst1::kanMX6 Δmrc1::ura4+ leu1::nmt-mst1L-S-leu1+ ura4-D18 ade6-M210 leu1-32*	This study
FY5304	*h+ Δmst1::kanMX6 leu1::nmt-mst1L-S-leu1+ exo1::ura4+ ura4-D18 leu1-32*	This study
FY5311	*h+ pht1-4KtoR-3HA-KanMX6 ura4-D18 leu1-32 ade6-M216 his3-D1*	Michael Keogh
FY6024	*h+ mst1-L344S-5FLAG:hphMX6 leu1-32 ura4-D18*	Eishi Noguchi
FY6229	*h- leu1-32 ura4-D18 ade6-M26 int::pUC8/ura4+/MATa/ade6-L469 his3-D1 ade6-M216*	Our stock
FY6632	*h- pku70::kanr his3-D1 ura4-D18 leu1-32 ade6-M216*	Our stock
FY8929	*h- mst1-L344S-5FLAG:hphMX6 leu1-32 ura4-D18 ade6-M26 int::pUC8/ura4+/MATa/ade6-L469 his3-D1 ade6-M216*	This study
FY9153	*h+ pht1::ura4 rad11-Cerulean::hphMX rad22-YFP-natMX leu1-32 ade6-M210 ura4-D18*	Our stock
FY9154	*h+ pht1-4KtoR-3HA-KanMX6 rad11-Cerulean::hphMX rad22-YFP-natMX ura4-D18 leu1-32 ade6-M216/210 his3-D1?*	This study
FY9338	*h- mst1-L344S-5FLAG:hphMX6 pku70::kanr rad11-Cerulean::hphMX rad22-YFP-natMX leu1-32 ura4-D18 his3-D1? ade6-M210*	This study
FY9352	*h- pku70::kanr rad11-Cerulean::hphMX rad22-YFP-natMX leu1-32 ura4-D18 his3-D1? ade6-M210*	This study
FY8989	*h- rad54-GFP:hphMX6*	Takuro Nakagawa
FY9023	*h- mst1-L344S-5FLAG:hphMX6 rad54-GFP:hphMX6 leu1-32? ura4-D18?*	This study
FY9340	*h- pku70::kanr rad54-GFP:hphMX6 leu1-32? his3-D1? ade6-M210?*	This study

FY9353	*h- mst1-L344S-5FLAG:hphMX6 pku70::kanr rad54-GFP:hphMX6 leu1-32? his3-D1? ade6-M210?*	This study
FY7479	*h- arg3::HOsite-natMX ars1::p41nmt1-HO(his3+) lys1-131::pdis1-mCherry-lacI(lys1+) erg7ter::lacO(ura4+) rad52-tandemCFP::kanMX leu1-32 his3-D1 ura4-294*	Li-Lin Du
FY8992	*h- mst1-L344S-5FLAG:hphMX6 arg3::HOsite-natMX ars1::p41nmt1-HO(his3+) lys1-131::pdis1-mCherry-lacI(lys1+) erg7ter::lacO(ura4+) rad52-tandemCFP::kanMX leu1-32 his3-D1 ura4-294/D18?*	This study
FY4620	*h- chk1HA(ep) cds1-myc::KanMX ade6-M216 ura4-D18 leu1-32*	Our stock
FY9495	*h+ exo1Δ::hph arg3::HOsite-natMX ars1::p41nmt1-HO(his3+) lys1-131::pdis1-mCherry-lacI(lys1+) erg7ter::lacO(ura4+) rad52-tandemCFP::kanMX leu1-32 his3-D1 ura4-294*	This study
FY9499	*h- pku70::kanr arg3::HOsite-natMX ars1::p41nmt1-HO(his3+) lys1-131::pdis1-mCherry-lacI(lys1+) erg7ter::lacO(ura4+) rad52-tandemCFP::kanMX leu1-32 his3-D1 ura4-294/D18 ade6-M210?*	This study
FY9502	*h- pht1-4KtoR-3HA-KanMX6 arg3::HOsite-natMX ars1::p41nmt1-HO(his3+) lys1-131::pdis1-mCherry-lacI(lys1+) erg7ter::lacO(ura4+) rad52-tandemCFP::kanMX leu1-32 his3-D1 ura4-294/D18?*	This study
FY9514	*h+ exo1Δ::hph mst1-L344S-5FLAG:hphMX6 arg3::HOsite-natMX ars1::p41nmt1-HO(his3+) lys1-131::pdis1-mCherry-lacI(lys1+) erg7ter::lacO(ura4+) rad52-tandemCFP::kanMX leu1-32 his3-D1 ura4-294*	This study
FY9542	*h- pku70::kanr mst1-L344S-5FLAG:hphMX6 arg3::HOsite-natMX ars1::p41nmt1-HO(his3+) lys1-131::pdis1-mCherry-lacI(lys1+) erg7ter::lacO(ura4+) rad52-tandemCFP::kanMX leu1-32 his3-D1 ura4-294/D18 ade6-M210?*	This study
FY5083	*h- Δmst1::kanMX6 leu1::nmt-mst1L-S-leu1+ chk1HA(ep) cds1-myc::KanMX ura4-D18 ade6-M210/216?*	This study
FY3397	*h- leu1-32 ura4-D18 ade6-M210 his3-D1 hta1-S129A:ura4+ hta2-S128A:his3+*	Takuro Nakagawa
FY5548	*h- ura4-D18 leu1-32 his3-D1 ade6-M210 mst1::[mst1-V5 leu1+] rad22-YFP::hphMX arg3::HOsite(KanMX4) ars1::nmt41-HOendonuclease:ampR:his3+:ars1*	Our stock
FY9561	*h- clr4::kanMX6-Bioneer mst1::[mst1-V5 leu1+] rad22-YFP::hphMX arg3::HOsite(KanMX4) ars1::nmt41-HOendonuclease:ampR:his3+:ars1his3-D1 ura4-D18 leu1-32 ade6-M210*	This study